JOURNAL OF TISSUE ENGINEERING AND REGENERATIVE MEDICINE
J Tissue Eng Regen Med (2011).
Published online in Wiley Online Library (wileyonlinelibrary.com) **DOI:** 10.1002/term.379

RESEARCH ARTICLE

Osteogenic potential of rat stromal cells derived from periodontal ligament

Tomotaka Kato[1,2], Koji Hattori[2]*, Tomonori Deguchi[2], Yoshihiro Katsube[2], Tomohiro Matsumoto[2,3], Hajime Ohgushi[2] and Yukihiro Numabe[1]

[1]*Nippon Dental University, School of Life Dentistry at Tokyo, Department of Periodontology, Tokyo, Japan*
[2]*Health Research Institute, National Institute of Advanced Industrial Science and Technology, Amagasaki Site, Amagasaki, Hyogo, Japan*
[3]*Tsurumi University, School of Dentistry, Department of Oral Surgery, Yokohama, Kanagawa, Japan*

Abstract

Various mesenchymal stromal cells (MSCs) have been applied to regenerative medicine. MSCs derived from periodontal tissue could also be a useful cell source for alveolar bone regeneration. However, only a few attempts of direct comparisons have been made between MSCs from periodontal tissues and those from other somatic tissues. The purpose of this study was to clarify the osteogenic characteristics of mesenchymal stromal cells derived from bone marrow (BMSCs), adipose tissue (ASCs) and periodontal ligament (PDLSCs). BMSCs, ASCs and PDLSCs were isolated from Fisher 344 rats. After 1 week of primary culture, stromal cells were subjected to cell surface analysis and osteogenic differentiation. The cells were subcultured for 2 weeks with and without osteogenic supplements (OS), followed by biochemical and histological analyses. With regard to cell surface antigens, all MSCs were positive for CD29 and CD90 and negative for CD45. With regard to osteogenic differentiation, BMSCs with OS had the highest ALP activity, calcium uptake and osteocalcin content. Without OS, PDLSCs had the highest levels of these bone differentiation markers. RT–PCR analysis and histological analysis showed similar trends. These results indicate that PDLSCs are an ideal candidate for alveolar bone regeneration. Copyright © 2011 John Wiley & Sons, Ltd.

Received 5 May 2010; Accepted 2 September 2010

Keywords **mesenchymal stromal cells; periodontal ligament; bone marrow; adipose tissue; osteogenesis; tissue engineering**

1. Introduction

Mesenchymal stromal cells (MSCs) are fibroblast-like cells that can be isolated from a variety of tissues, such as bone marrow (Pittenger *et al.*, 1999), periosteum (De Bari *et al.*, 2001a), synovium (De Bari *et al.*, 2001b) and adipose tissue (Zuk *et al.*, 2002). MSCs include multipotent stem cells; therefore, various MSCs have been applied to regenerative medicine. Bone marrow-derived MSCs (BMSCs) can differentiate into multiple lineages, such as osteoblasts, adipocytes, chondrocytes and hepatocytes (Pittenger *et al.*, 1999; Kotobuki *et al.*, 2004). In clinical practice, tissue-engineering methods using BMSCs have been applied to the regenerative cell therapy of bone, articular cartilage, liver, neurons and cardiovascular diseases (Ohgushi *et al.*, 1999). Adipose-derived MSCs (ASCs) have also been used to treat various diseases, including the treatment of widespread traumatic calvarial defects (Lendeckel *et al.*, 2004), cosmetic breast augmentation (Yoshimura *et al.*, 2008) and rectovaginal fistula in perianal Crohn's disease (García-Olmo *et al.*, 2010). Moreover, MSCs from synovial tissue and umbilical cord blood have been shown to be promising alternative sources of MSCs (Rosenbaum *et al.*, 2008).

In the periodontal field, the periodontal ligament, which is a soft connective tissue embedded between the cementum and the inner wall of the alveolar bone socket, contains heterogeneous cell populations that can differentiate multiple lineages (Seo *et al.*, 2004; Iwata *et al.*, 2009). Therefore, periodontal ligament-derived MSCs (PDLSCs) are also expected to be a useful cell

*Correspondence to: Koji Hattori, Health Research Institute, National Institute of Advanced Industrial and Technology, Amagasaki Site, 3-11-46 Nakoji, Amagasaki, Hyogo 661-0974, Japan. E-mail: koji-hattori@aist.go.jp

source for alveolar bone regeneration (Seo *et al.*, 2004). At present, BMSCs, ASCs and PDLSCs are used for alveolar bone regeneration (Yamada *et al.*, 2006; Tobita *et al.*, 2008; Iwata *et al.*, 2009); however, only a few attempts at direct comparison (Lindroos *et al.*, 2008) have been made between PDLSCs and those from other somatic tissues under the same culture conditions, including the same donor tissue, passage number and culture environment. The purpose of this study was to clarify the osteogenic characteristics of BMSCs, ASCs and PDLSCs.

2. Materials and methods

2.1. Preparation and culture of rat BMSCs, ASCs and PDLSCs

We harvested BMSCs, ASCs and PDLSCs from 12 week-old Fischer 344 male rats purchased from Japan SLC (Shizuoka, Japan). All procedures used in the animal experiments conform with the Guidelines for the Care and Use of Laboratory Animals of the National Institute of Advanced Industrial Science and Technology of Japan. Three rats were sacrificed using 2% halothane (Takeda Pharmaceuticals, Osaka, Japan) in a glass jar.

BMSCs were isolated as described previously (Hayashi *et al.*, 2008). Briefly, both ends of the femora were cut away from the epiphysis and marrow was flushed out using 10 ml culture medium expelled from a syringe through a 20 gauge needle. The released bone marrow cells were collected in a T-75 flask for primary culture. ASC isolation was performed as described previously (Hayashi *et al.*, 2008). Briefly, rat inguinal adipose tissue was treated with 10 ml phosphate-buffered saline (PBS) containing 3 mg/ml collagenase (Wako Pure Chemical Industries, Osaka, Japan) for 1 h, followed by centrifugation at 400 × *g* for 5 min after filtration through 40 μm cell strainers. The sediment was resuspended in culture medium and isolated adipose cells were collected in a T-75 flask for primary culture. PDLSC isolation was performed as described by Techawattanawisal *et al.* (2007), with some modifications. Briefly, rat maxillary and mandibular molars (M1, M2 and M3) were washed with PBS containing 5% antibiotics. Under microscopic inspection, the gingiva was carefully exfoliated and maxillary and mandibular molars were removed from the sockets using extraction forceps. The extracted molars were washed twice with PBS containing 5% antibiotics. Subsequently, these molars were treated with 10 ml PBS containing 3 mg/ml collagenase for 1 h. The digest was then centrifuged at 400 × *g* for 5 min following filtration with 40 μm cell strainers. The sediment was resuspended in culture medium. From 10 molars, 4×10^5 periodontal cells were isolated and collected in a T-75 flask for primary culture.

Primary cultures of BMSCs, ASCs and PDLSCs were maintained in a humidified atmosphere of 95% air and 5% CO_2 at 37 °C. In primary cultures, the medium was renewed three times/week. After 1 week of primary culture, cells were released from the substratum using trypsin–EDTA (0.05% trypsin, 0.53 mM EDTA-4Na; Invitrogen, Carlsbad, CA, USA) and were subjected to analysis of cell surface, proliferation rates and osteogenic differentiation.

2.2. Cell surface analysis

Harvested cells were suspended at 1×10^6 cells/ml in PBS. Cell suspensions (100 μl) were placed into 1.5 ml centrifuge tubes and incubated with anti-CD antibodies on ice for 20 min. PBS containing 10% Block Ace (Dainippon Pharmaceutical Co. Ltd, Osaka, Japan) was then added to the tubes, followed by analysis using a FACSCalibur flow cytometer (BD). The antibodies used were CD29-FITC (fluorescein isothiocyanate), CD90-FITC and CD45-FITC (BioCarta Inc., San Diego, CA, USA). Mouse IgG-FITC (Beckman Coulter) was used as a negative control.

2.3. Cell proliferation rates

Cell proliferation rates of BMSCs, ASCs and PDLSCs were compared on the measurement of 5-bromo-2′-deoxyuridine (BrdU) incorporation, using an Amersham Cell Proliferation Biotrak ELISA System (GE Healthcare, Buckinghamshire, UK). After primary cultures, BMSCs, ASCs and PDLSCs were plated at 10^4 cells/well in 96-well plates and cultured for 24 h. BrdU labelling solution was added to the culture wells and incubated for 4 h. After fixing and blocking for 30 min, peroxidase-labelled anti-BrdU was added and incubated for 1 h, thenBrdU incorporation was measured using a microplate reader (Wallac 1420 ARVOsx; Perkin-Elmer, Boston, MA, USA).

2.4. *In vitro* osteogenic differentiation

After primary culture, BMSCs, ASCs and PDLSCs were subcultured for 2 weeks in 12-well tissue culture plates at a cell density of $2.0 \times 10^4/\text{cm}^2$ for histochemical staining and RT–PCR analysis, and in 24-well tissue culture plates at a cell density of $1.0 \times 10^4/\text{cm}^2$ for biochemical analyses. Under non-differentiation conditions, medium supplemented with 10 mM β-glycerophosphate (Calbiochem, San Diego, CA, USA) and 0.28 mM ascorbic acid-2-phosphate (Wako Pure Chemical Industries, Osaka, Japan) was renewed three times/week. Under osteogenic differentiation conditions, the medium was further supplemented with 10 nM dexamethasone (Nacalai Tesque, Kyoto, Japan).

2.5. Histochemical staining

After washing twice with PBS, the cultured cells were fixed in 10% paraformaldehyde and then were stained with alizarin red S (Sigma-Aldrich, St Louis, MO, USA) for 2 min, followed by ALP staining for 5 min. ALP staining

was performed as described previously (Ohgushi *et al.*, 1996).

2.6. Mineralization analysis by calcein uptake

To visualize the mineralized extracellular matrix of subcultured cells, the calcein uptake assay according to our previous report was performed (Uchimura *et al.*, 2003). For the calcein assay, 1 μg/ml calcein was added to each well whenever the culture medium was renewed. Prior to the assays, subcultured cell layers were washed twice with PBS. After 2 weeks of culture, calcein incorporated into the mineralization of the matrix was observed using a fluorescence microscope (Model IX70, Olympus, Tokyo, Japan) and was visualized and quantified using a Typhoon 8600 image analyser (Molecular Dynamics, Sunnyvale, CA, USA).

2.7. Measurements of ALP activities

ALP activity and DNA content were measured as described previously (Ohgushi *et al.*, 1996). The layers of subcultured cells were washed twice with PBS and were collected by scraping into sample tubes containing 500 μl 10 mM Tris buffer (pH 7.4, 1 mM EDTA and 100 mM NaCl). The samples were sonicated and used for DNA quantification. Quantification of DNA contents was performed using Hoechst 33 258 (Invitrogen). The sonicated suspension (20 μl) was mixed with 200 μl 0.25 μg/ml Hoechst 33 258 and incubated for 5 min at room temperature. Fluorescence was measured on the microplate reader. Standard DNA was prepared with salmon sperm DNA (Invitrogen). The remnant suspension was used for measurement of ALP activity. After centrifuging at 12 000 × *g* for 3 min at 4 °C, 20 μl supernatant was mixed with 100 μl *p*-nitrophenylphosphate substrate, followed by incubation for 30 min at 37 °C. The ALP activity represented by the amount of *p*-nitrophenol release was normalized against the DNA content. The remaining supernatant, including the sonicated cell suspension, was used for the osteocalcin assay.

2.8. Quantification of osteocalcin

After ALP measurements, 300 μl 20% formic acid was added to the tube in order to extract inorganic ions and organic matrix proteins, and the samples were stored at 4 °C for 48 h. The samples were then centrifuged at 15 000 × *g* for 10 min at 4 °C. Gel filtration was applied to the supernatant in order to eliminate inorganic ions, after which gel-filtered samples were evaporated. The resulting concentrated samples were added to an enzyme immunoassay plate immobilized with anti-rat osteocalcin antibodies in order to measure the concentrations of osteocalcin with an intact rat osteocalcin enzyme immunoassay kit (Biomedical Technologies, Stoughton, MA, USA).

2.9. Semi-quantification of mRNAs by RT–PCR analysis

After 2 weeks of subculture, total RNA was isolated from the cell layers using an RNeasy Mini kit (Qiagen, Hilden, Germany). Total RNA was reverse-transcribed using ReverTra Ace (Toyobo, Osaka, Japan) in a 20 μl reaction volume. Gene-specific amplicons were then amplified by polymerase chain reaction (PCR). Semi-quantitative RT–PCR was performed for *osteocalcin*. Glyceraldehyde-3-phosphate dehydrogenase (*GAPDH*) was used as a control housekeeping gene (Gartland *et al.*, 2005). The PCR primers were as follows (forward and reverse, 5′ to 3′): *osteocalcin*, CATGAGGACCCTCTCTCTCTGC and CCTAAACGGTGGTGCCATAG; *GAPDH*, AACTCC-CTCAAGATTGTTCAGCA and TCCACCACCCTGTTGGCT-GTA. PCR conditions were as follows: 94 °C for 30 s, 60 °C for 30 s, 72 °C for 40 s for 30 cycles.

2.10. Statistical analysis

Statistical analyses were performed using the Excel Statistical Program File Ystat 2008 (developed by Yamazaki S, Igakutosyo Syuppan Co. Ltd, Tokyo, Japan). Calcein, ALP activity and osteocalcin contents were analysed by one-way repeated analysis of variance (ANOVA). In all analyses, the significance level was set at $p < 0.01$.

3. Results

3.1. Cell morphology, surface analysis and proliferation rates

BMSCs, ASCs and PDLSCs became largely confluent in T-75 flasks after 1 week of primary culture. These cells exhibited fibroblastic morphology, which is characteristic of MSCs (Figure 1A). Cell surface markers for rat MSCs are not as well understood as human MSCs. Therefore, cell surface markers were selected with reference to the literature (Figure 1B). All three cell types were positive for markers present in mesenchymal cells (CD29 and CD90) and were negative for haematopoietic markers (CD31, CD44, CD45 and CD172; data for CD31, CD44 and CD172 are not shown in the Figure). Therefore, all three cell types showed similar cell surface antigens and were mesenchymal cells (Nagaya *et al.*, 2004). The proliferation rates of three MSC types were compared on the BrdU (Figure 1C). As shown the figure, proliferation rates were different for each of MSCs. Although the proliferation rate of the PDLSCs was low compared with other cell types, the PDLSCs together with other cells become almost confluent after 1week. Therefore, a

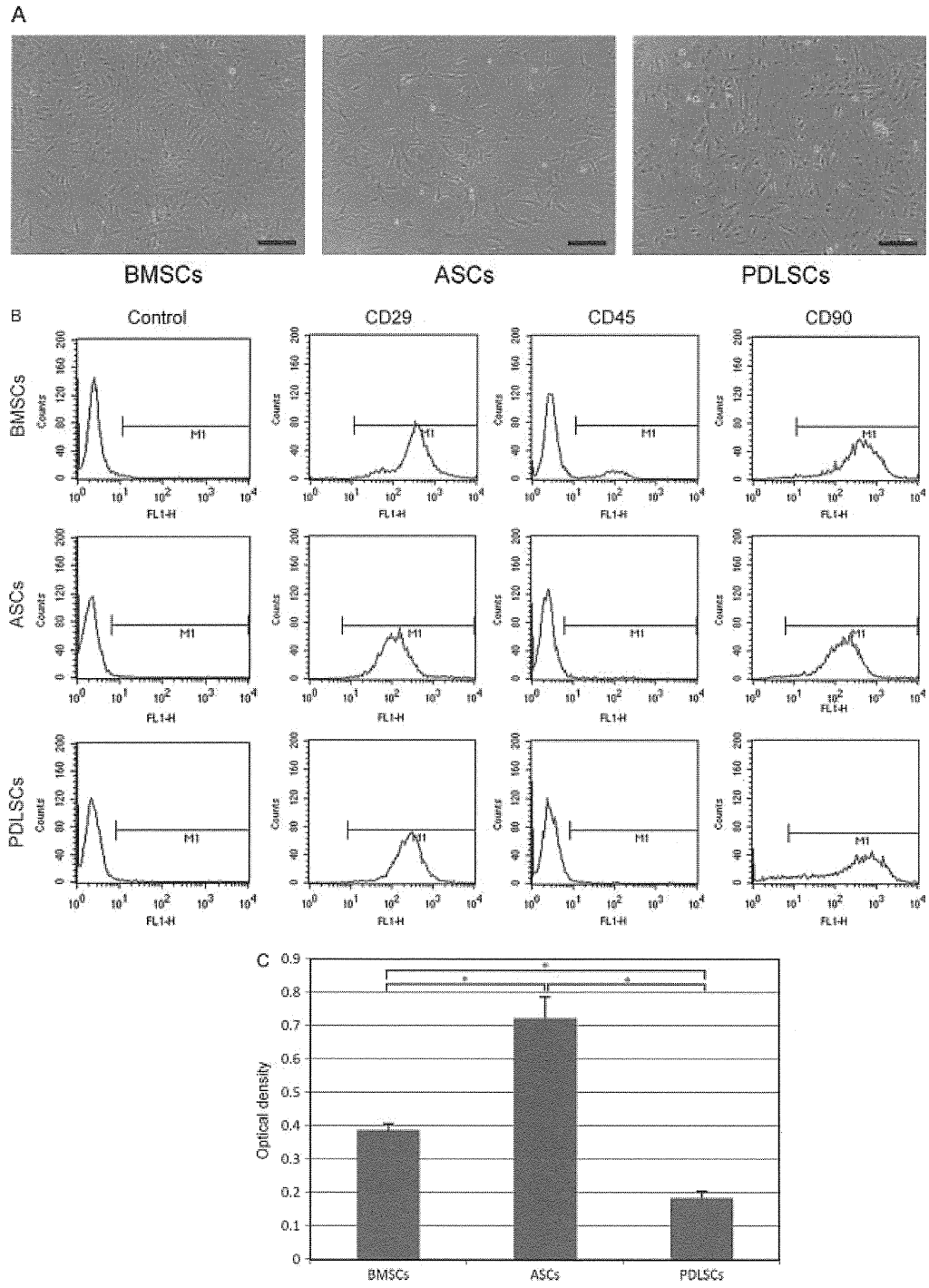

Figure 1. Characteristics of primary cultured MSCs. (A) Phase-contrast micrographs of BMSCs, ASCs and PDLSCs after 1 week of primary culture (scale bar = 200 μm). (B) Cell surface analysis of BMSCs, ASCs and PDLSCs after 1 week of primary culture. Brackets indicate positive cell population. BMSCs, ASCs and PDLSCs showed similar profiles; positive for CD29 and CD90 and negative for CD45. (C) Cell proliferation of BMSCs, ASCs and PDLSCs measured by BrdU incorporation. Values are means ± SD ($n = 8$). $^*p < 0.01$ (one-way ANOVA)

sufficient number of cells was obtained using the culture method as described above.

3.2. Histochemical staining

Histochemical staining for BMSCs, ASCs and PDLSCs was performed after 2 weeks of subculture under osteogenic differentiation and non-differentiation conditions (Figure 2A). Under non-differentiation conditions, ALP staining was noted on BMSCs and PDLSCs, while alizarin red S-positive nodules were only seen in PDLSCs. Under osteogenic differentiation conditions, ALP staining was noted on BMSCs and PDLSCs, while alizarin red S-positive nodules were seen in BMSCs and PDLSCs. As shown in Figure 3, ALP and alizarin red S staining was

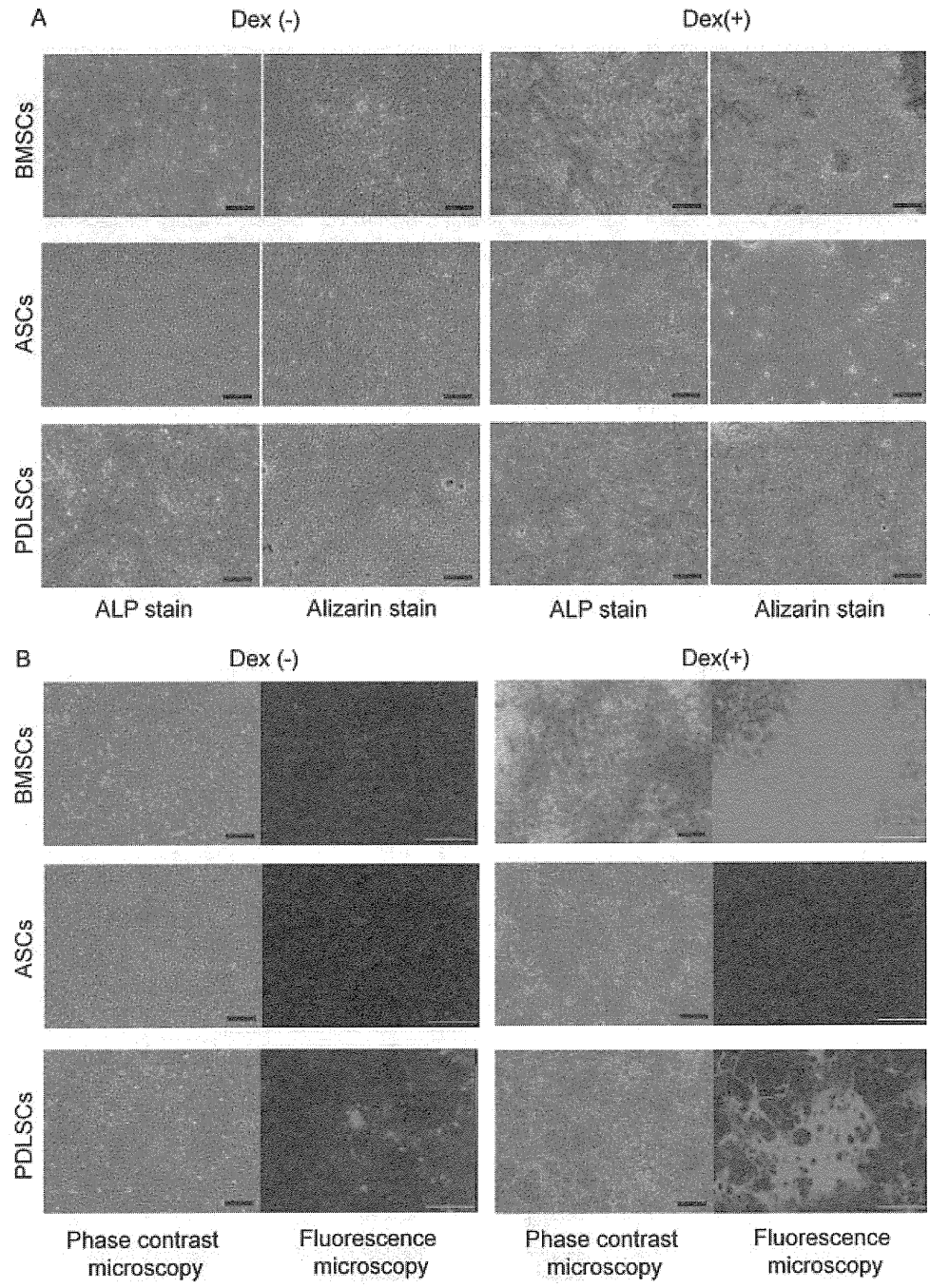

Figure 2. Histochemical staining. (A) ALP and alizarin red S staining under non-differentiation and osteogenic differentiation conditions (scale bar = 200 μm). (B) Phase-contrast micrographs and fluorescence micrographs of BMSCs, ASCs and PDLSCs under non-differentiation and osteogenic differentiation conditions (scale bar = 200 μm). Phase-contrast micrographs show extracellular bone mineral regions (brown areas). Fluorescence micrographs show calcein uptake (green areas)

more intense for BMSCs than PDLSCs. However, ALP staining and alizarin red S-positive nodules were not seen in ASCs under either non-differentiation or osteogenic differentiation conditions.

3.3. Calcein staining, quantification of mineralization and calcein uptake

In order to quantitatively analyse the mineralization of BMSCs, ASCs and PDLSCs, calcein, which is a calcium-binding fluorescent dye, was added to the culture medium. The calcein fluorescence intensities in the mineralized matrix of BMSCs, ASCs and PDLSCs were assessed 2 weeks after subculture. Under non-differentiation conditions, numerous fluorescent spots were noted on the PDLSCs and faint fluorescent spots could be detected in the BMSCs (Figure 2B). Under osteogenic differentiation conditions, fluorescence could be detected in PDLSCs and BMSCs. The fluorescence was more intense and extensive in BMSCs than in PDLSCs. The quantitative data for the fluorescence intensities

DOI: 10.1002/term

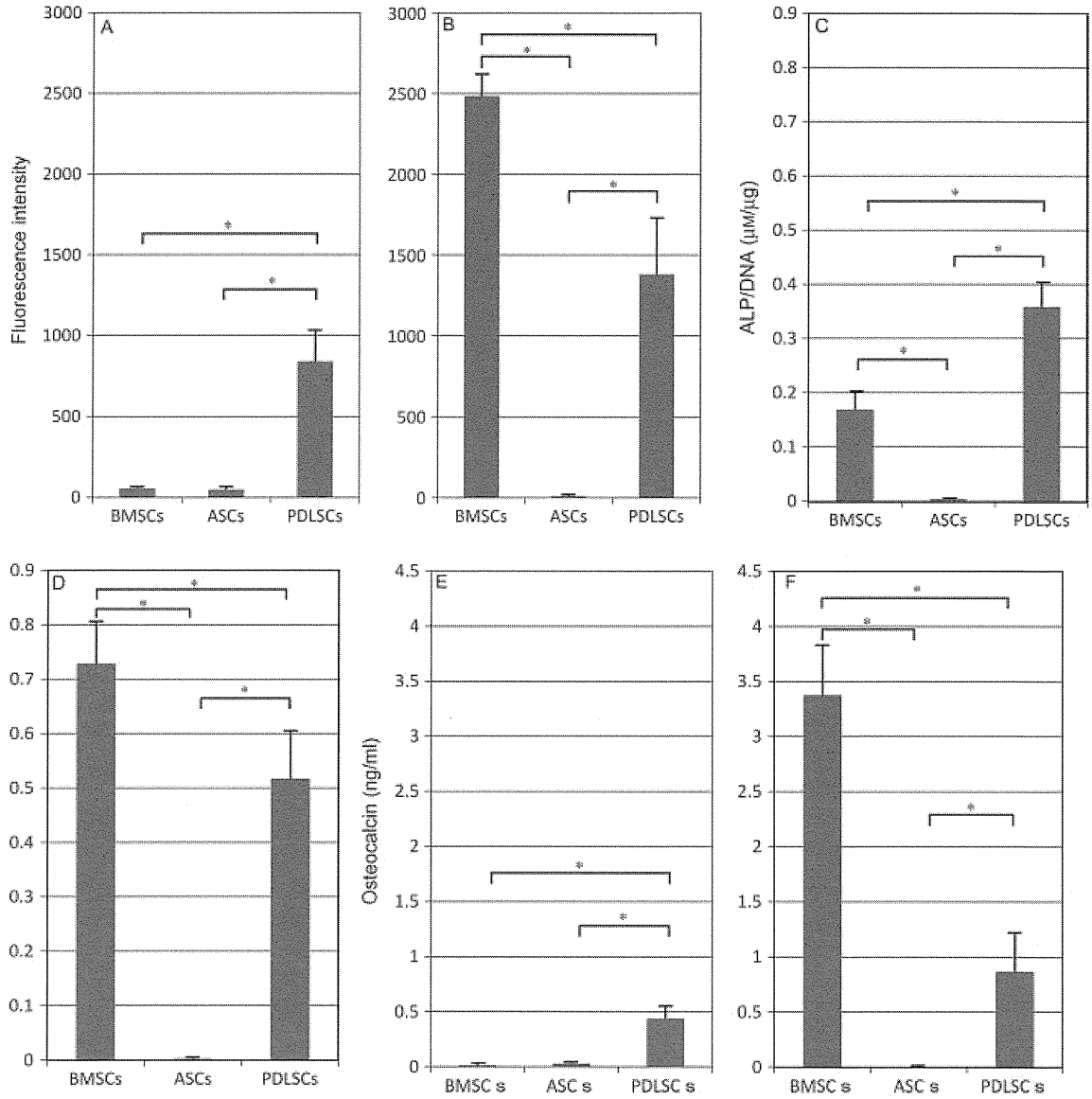

Figure 3. Quantification of osteoblastic markers. (A) Calcein uptake (fluorescence intensity) of BMSCs, ASCs and PDLSCs under non-differentiation and (B) osteogenic differentiation conditions. Values are means ± SD ($n = 6$). $^*p < 0.01$ (one-way ANOVA). (C) ALP activity of BMSCs, ASCs and PDLSCs under non-differentiation and (D) osteogenic differentiation conditions. Values are means ± SD ($n = 6$). $^*p < 0.01$ (one-way ANOVA). (E) Osteocalcin contents in BMSCs, ASCs and PDLSCs under non-differentiation and (F) osteogenic differentiation conditions. Values are means ± SD ($n = 6$). $^*p < 0.01$ (one-way ANOVA)

are shown in Figure 3A, B. Under non-differentiation conditions, the fluorescence intensity of PDLSCs was highest among the three cell types (Figure 3A). Significant differences were observed between PDLSCs and other MSCs. Under osteogenic differentiation conditions, the fluorescence intensity of BMSCs was highest among the three cell types (Figure 3B). In contrast to BMSCs and PDLSCs, ASCs demonstrated remarkably low fluorescence intensity under either osteogenic differentiation or non-differentiation conditions.

3.4. Quantification of ALP activity

ALP activity is recognized as an early osteoblastic marker. The ALP activity of each sample was normalized against the DNA content of the cells in the sample. Under non-differentiation conditions, ALP activity of PDLSCs was highest among the three cell types (Figure 3C). Under osteogenic differentiation conditions, the ALP activity of BMSCs was highest among the three cell types (Figure 3D). Significant differences were observed between all pairs of three cell types under either osteogenic differentiation or non-differentiation conditions.

3.5. Quantification of osteocalcin and RT–PCR analysis

Osteocalcin is known to be a bone-specific protein and is used as a late marker of osteogenic differentiation. We analysed the osteocalcin contents of cultured cell layers

DOI: 10.1002/term

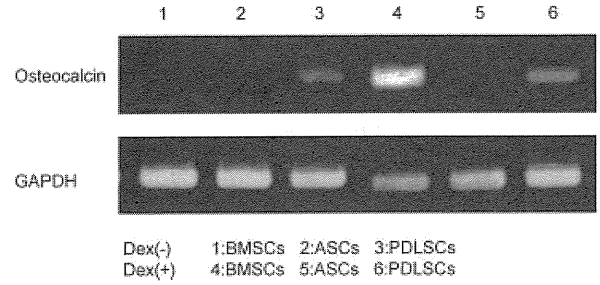

Figure 4. Osteocalcin and *GAPDH* gene expression by RT–PCR analysis

and mRNA expression levels were assessed after 2 weeks of subculture under non-differentiation and osteogenic differentiation conditions. The results for osteocalcin contents showed the same trend as calcein uptake and ALP activity. Under non-differentiation conditions, osteocalcin contents in PDLSCs were the highest among the three cell types (Figure 3E). Significant differences were observed between PDLSCs and other MSCs. Under osteogenic differentiation conditions, the osteocalcin contents of BMSCs were highest among the three cell types (Figure 3F). Significant differences were observed between all pairs of three cell types. RT–PCR analysis confirmed osteocalcin expression in PDLSCs under non-differentiation conditions and in BMSCs and PDLSCs under osteogenic differentiation conditions (Figure 4). Higher levels of osteocalcin expression of were confirmed in BMSCs when compared with PDLSCs under osteogenic differentiation conditions.

4. Discussion

In this study, we performed a direct comparison of three MSC types. On cell surface analysis, the three types of cell had similar characteristics at the end of primary culture, i.e. the three cell types had the same cell surface antigens and were of the mesenchymal type. After subculture, osteogenic supplements were shown to stimulate osteogenic differentiation of both BMSCs and PDLSCs. In addition, BMSCs had a higher osteogenic potential than PDLSCs. Under non-differentiation conditions, only PDLSCs showed osteogenic potential. However, ASCs demonstrated remarkably low osteogenic potential under either osteogenic differentiation or non-differentiation conditions. Our observations agreed with the results of other studies (Yoshimura *et al.*, 2007; Hayashi *et al.*, 2008). Therefore, BMSCs and PDLSCs are apparently ideal candidates for alveolar bone regeneration.

In 1982, guided tissue regeneration (GTR) was first applied to the regeneration of alveolar bone (Nyman *et al.*, 1982) and several surgical treatments have since been developed for the regeneration of periodontal tissue (Sculean *et al.*, 2008). GTR is a surgical procedure that utilizes a barrier membrane to direct the growth of periodontal ligament- and bone-derived cells, including bone. The principle is that the barrier membrane excludes unwanted cells from the healing site in order to allow growth of the desired tissue. According to the accumulated clinical data (Yamada *et al.*, 2006; Okuda *et al.*, 2009), research began to focus on the regeneration of new bone in an area where teeth are being extracted or have already been removed. Therefore, osteogenic cells from extracted teeth could be a useful tool for alveolar bone regeneration.

In this study we investigated the osteogenic characteristics of BMSCs, ASCs and PDLSCs and we demonstrated the osteogenic potential of BMSCs and PDLSCs. BMSCs are well-known multipotent cells that differentiate into adipocytes, chondrocytes and osteoblasts (Pittenger *et al.*, 1999). For bone regeneration using BMSCs, surgical stress (discomfort caused by bone marrow extraction) is induced when harvesting bone marrow, and osteogenic supplements may be required for osteoblastic differentiation. In contrast, PDLSCs can be expanded from extracted teeth, which are typically discarded, and have osteogenic potential without dexamethasone. Therefore, both PDLSCs and BMSCs are candidates for utilization in alveolar bone regeneration.

Although several studies have focused on the osteogenic potential of ASCs, there remains some controversy. Im *et al.* (2005) showed that human ASCs have inferior osteogenic capability when compared to BMSCs (Im *et al.*, 2005). Hayashi *et al.* (2008) reported that rat BMSCs showed distinct osteogenic differentiation capacity when compared with rat ASCs *in vivo* and *in vitro*. In contrast, De Ugarte *et al.* (2003) found no significant differences in osteogenic capacity between human BMSCs and ASCs. However, Im Gl *et al.* and De Ugarte *et al.* used human MSCs that had been passaged more than three times and ALP activity levels of human MSCs are very low when compared with the present study. Moreover, ALP activity analysis of human MSCs has low statistical power (Hayashi *et al.*, 2008). In rat ASCs, some studies show osteogenic capacity (Yoshimura *et al.*, 2007); however, these authors also used MSCs that had been passaged more than twice. Tobita *et al.* (2008) revealed that ASCs mixed with platelet-rich plasma can regenerate periodontal tissue, including alveolar bone. Therefore, for the osteogenic differentiation of ASCs, more osteogenic supplements in addition to dexamethasone may be required.

Dexamethasone is a steroid drug and acts as an anti-inflammatory and immunosuppressant. In bone tissue-engineering fields, dexamethasone has been used to promote undifferentiated stem cells to differentiate in the osteogenic lineage. However, the mechanism of osteogenic differentiation is not clear. In our study, BMSCs showed distinct osteogenic differentiation capability compared with PDLSCs under osteogenic differentiation conditions with dexamethasone. In contrast to BMSCs, PDLSCs showed osteogenic potential even under non-differentiation conditions. Based on these results, it is speculated that PDLSCs as a heterogeneous cell population contain many osteogenic cells and BMSCs contain many undifferentiated stem cells. The osteogenic property of the PDLSCs might show benefits for clinical

DOI: 10.1002/term

situations because of pre-existing osteogenic cells in their population. In this regard, Feng *et al.* (2010) utilized cultured PLDSCs under non-differentiation conditions for three patients with periodontitis. They demonstrated the clinical, experimental evidences to supporting an efficacy and safety of PLDSCs transplantation.

In conclusion, we have demonstrated the utility of PDLSCs for periodontal bone regeneration. Seo *et al.* (2004) confirmed the multipotency of PDLSCs, which differentiate into cementoblast-like cells, adipocytes and collagen-forming cells). Therefore, PDLSCs are potentially useful for periodontal tissue regeneration. Due to their durability after freezing, cryopreserved PDLSCs may also become an ideal candidate for utilization in periodontal tissue regeneration (Oh *et al.*, 2005; Seo *et al.*, 2005).

Acknowledgements

We appreciate the advice and expertise of Mika Tadokoro and we thank our many colleagues for their support during this present study. This work was supported in part by the Project for Realization of Regenerative Medicine from the Ministry of Education, Culture, Sports, Science and Technology of Japan. The study sponsors had no role in the study design, data analysis or data interpretation, or in the writing of the report.

References

De Bari C, Dell'Accio F, Luyten FP. 2001; Human periosteum-derived cells maintain phenotypic stability and chondrogenic potential throughout expansion regardless of donor age. *Arthritis Rheum* **44**: 85–95.

De Bari C, Dell'Accio F, Tylzanowski P, *et al.* 2001; Multipotent mesenchymal stem cells from adult human synovial membrane. *Arthritis Rheum* **44**: 1928–1942.

De Ugarte DA, Morizono K, Elbarbary A, *et al.* 2003; Comparison of multi-lineage cells from human adipose tissue and bone marrow. *Cells Tissues Organs* **174**: 101–109.

Feng F, Akiyama K, Liu Y, *et al.* 2010; Utility of PDL progenitors for *in vivo* tissue regeneration: a report of three cases. *Oral Dis* **16**: 20–28.

García-Olmo D, Herreros D, De-La-Quintana P, *et al.* 2010; Adipose-derived stem cells in Crohn's rectovaginal fistula. *Case Report Med* **2010**: 961758.

Gartland A, Mechler J, Mason-Savas A, *et al.* 2005; *In vitro* chondrocyte differentiation using costochondral chondrocytes as a source of primary rat chondrocyte cultures: an improved isolation and cryopreservation method. *Bone* **37**: 530–544.

Hayashi O, Katsube Y, Hirose M, *et al.* 2008; Comparison of osteogenic ability of rat mesenchymal stem cells from bone marrow, periosteum, and adipose tissue. *Calcif Tissue Int* **82**: 238–247.

Im Gl, Shin YW, Lee KB. 2005; Do adipose tissue-derived mesenchymal stem cells have the same osteogenic and chondrogenic potential as bone marrow-derived cells? *Osteoarthr Cartilage* **13**: 845–853.

Iwata T, Yamato M, Tsuchioka H, *et al.* 2009; Periodontal regeneration with multi-layered periodontal ligament-derived cell sheets in a canine model. *Biomaterials* **30**: 2716–2723.

Kotobuki N, Hirose M, Takakura Y, *et al.* 2004; Cultured autologous human cells for hard tissue regeneration: preparation and characterization of mesenchymal stem cells from bone marrow. *Artif Organs* **28**: 33–39.

Lendeckel S, Jödicke A, Christophis P, *et al.* 2004; Autologous stem cells (adipose) and fibrin glue used to treat widespread traumatic calvarial defects: case report. *J Craniomaxillofac Surg* **32**: 370–373.

Lindroos B, Mäenpää K, Ylikomi T, *et al* 2008; Characterisation of human dental stem cells and buccal mucosa fibroblasts. *Biochem Biophys Res Commun* **368**: 329–335.

Nagaya N, Fujii T, Iwase T, *et al.* 2004; Intravenous administration of mesenchymal stem cells improves cardiac function in rats with acute myocardial infarction through angiogenesis and myogenesis. *Am J Physiol Heart Circ Physiol* **287**: 2670–2676.

Nyman S, Lindhe J, Karring T, *et al.* 1982; New attachment following surgical treatment of human periodontal disease. *J Clin Periodontol* **9**: 290–296.

Oh H-Y, Che M-Z, Hong C-J, *et al.* 2005; Cryopreservation of human teeth for future organization of a tooth bank: a preliminary study. *Cryobiology* **51**: 322–329.

Ohgushi H, Caplan AI. 1999; Stem cell technology and bioceramics: from cell to gene engineering. *J Biomed Mater Res* **48**: 913–927.

Ohgushi H, Dohi Y, Katuda T, *et al.* 1996; *In vitro* bone formation by rat marrow cell culture. *J Biomed Mater Res* **32**: 333–340.

Pittenger MF, Mackay AM, Beck SC, *et al.* 1999; Multilineage potential of adult human mesenchymal stem cells. *Science* **284**: 143–147.

Rosenbaum AJ, Grande DA, Dines JS. 2008; The use of mesenchymal stem cells in tissue engineering: a global assessment. *Organogenesis* **4**: 23–27.

Sculean A, Nikolidakis D, Schwarz F. 2008; Regeneration of periodontal tissues: combinations of barrier membranes and grafting materials – biological foundation and preclinical evidence: a systematic review. *J Clin Periodontol* **35**: 106–116.

Seo BM, Miura M, Gronthos S, *et al.* 2004; Investigation of multipotent postnatal stem cells from human periodontal ligament. *Lancet* **364**: 149–155.

Seo BM, Miura M, Sonoyama W, *et al.* 2005; Recovery of stem cells from cryopreserved periodontal ligament. *J Dent Res* **84**: 907–912.

Techawattanawisal W, Nakahama K, Komaki M, *et al.* 2007; Isolation of multipotent stem cells from adult rat periodontal ligament by neurosphere-forming culture system. *Biochem Biophys Res Commun* **357**: 917–923.

Tobita M, Uysal AC, Ogawa R, *et al.* 2008; Periodontal tissue regeneration with adipose-derived stem cells. *Tissue Eng A* **14**: 945–953.

Uchimura E, Machida H, Kotobuki N, *et al.* 2003; *In situ* visualization and quantification of mineralization of cultured osteogenetic cells. *Calcif Tissue Int* **73**: 575–583.

Yamada Y, Ueda M, Hibi H, *et al.* 2006; A novel approach to periodontal tissue regeneration with mesenchymal stem cells and platelet-rich plasma using tissue engineering technology: a clinical case report. *Int J Periodont Restor Dent* **26**: 363–369.

Yoshimura H, Muneta T, Nimura A, *et al.* 2007; Comparison of rat mesenchymal stem cells derived from bone marrow, synovium, periosteum, adipose tissue, and muscle. *Cell Tissue Res* **327**: 449–462.

Yoshimura K, Sato K, Aoi N, *et al.* 2008; Cell-assisted lipotransfer for cosmetic breast augmentation: supportive use of adipose-derived stem/stromal cells. *Aesthet Plast Surg* **32**: 48–57.

Zuk PA, Zhu M, Ashjian P, *et al.* 2002; Human adipose tissue is a source of multipotent stem cells. *Mol Biol Cell* **13**: 4279–4295.

Human Cell (2011) 24:2–8
DOI 10.1007/s13577-010-0006-8

RESEARCH ARTICLE

Use of BAC array CGH for evaluation of chromosomal stability of clinically used human mesenchymal stem cells and of cancer cell lines

Soichiro Saito · Keiko Morita · Arihiro Kohara · Tohru Masui · Mari Sasao · Hajime Ohgushi · Takashi Hirano

Received: 8 September 2010 / Accepted: 16 October 2010 / Published online: 31 December 2010

Abstract Array-based comparative genomic hybridization (aCGH) using bacterial artificial chromosomes (BAC) is a powerful method to analyze DNA copy number aberrations of the entire human genome. In fact, CGH and aCGH have revealed various DNA copy number aberrations in numerous cancer cells and cancer cell lines examined so far. In this report, BAC aCGH was applied to evaluate the stability or instability of cell lines. Established cell lines have greatly contributed to advancements in not only biology but also medical science. However, cell lines have serious problems, such as alteration of biological properties during long-term cultivation. Firstly, we investigated two cancer cell lines, HeLa and Caco-2. HeLa cells, established from a cervical cancer, showed significantly increased DNA copy number alterations with passage time. Caco-2 cells, established from a colon cancer, showed no remarkable differences under various culture conditions. These results indicate that BAC aCGH can be used for the evaluation and validation of genomic stability of cultured cells. Secondly, BAC aCGH was applied to evaluate and validate the genomic stabilities of three patient's mesenchymal stem cells (MSCs), which were already used for their treatments. These three MSCs showed no significant differences in DNA copy number aberrations over their entire chromosomal regions. Therefore, BAC aCGH is highly recommended for use for a quality check of various cells before using them for any kind of biological investigation or clinical application.

Keywords Validation of cell line · BAC · BAC array CGH

S. Saito · K. Morita
Bioproduction Research Institute, National Institute of Advanced Industrial Science and Technology (AIST), Tsukuba, Japan

A. Kohara · T. Masui
Division of Bioresources, National Institute of Biomedical Innovation, Osaka, Japan

M. Sasao · H. Ohgushi
Health Research Institute, AIST, Tsukuba, Japan

T. Hirano (✉)
Collaboration Promotion Department, AIST, Central 6, 1-1-1 Higashi, Tsukuba, Ibaraki 305-8566, Japan
e-mail: hirano-takashi@aist.go.jp

T. Hirano
Okinawa Science and Technology Promotion Center, Uruma, Japan

Introduction

Comparative genomic hybridization (CGH) and array-based CGH (aCGH) can detect DNA copy number aberrations in the entire human genome [1, 2]. In fact, to detect DNA copy number aberrations, aCGH has been used to examine many cancers and cancer cell lines for diagnosis and prognosis [3–7]. Moreover, in Korea an aCGH chip was approved for use to diagnose hereditary diseases and inherent chromosomal disorders, such as Down syndrome and Turner's syndrome, which are caused by chromosomal aberrations [Korean Food and Drug Administration (KFDA; http://www.macrogen.com/eng/macrogen/press_list.jsp)]. Bacterial artificial chromosome (BAC) aCGH has attracted attention as a superior method for genome-wide analysis not only to detect DNA copy number aberrations, but also to evaluate hereditary chromosomal disorders.

In recent years, regenerative medicine using mesenchymal stem cells (MSCs) has received much attention

[8, 9]. However, safety issues concerning the MSC applications, especially with respect to tumorigenesis, remain to be solved [9–11]. The BAC aCGH method would be useful for the evaluation of chromosomal stability and instability, which are closely related to tumorigenesis.

In this study, we performed BAC aCGH to evaluate chromosomal stability of HeLa cells, Caco-2 cells, and MSCs. The HeLa cell line was established as the first human cancer cell line derived from a cervical cancer and is one of the most widely used cell lines in the world [12, 13]. However, numerous other established cell lines are now used as a substitute for HeLa cells [13]. The Caco-2 cell line was established from a human colon cancer [14]. Even though the Caco-2 cell was derived from a colon cancer, it has been available for use as a convenient reference model for theoretical predictions of intestinal drug absorption in drug discovery [15]. Therefore, the stability of Caco-2 cells should be established for such a screening purpose. MSCs are expected to be applied for regenerative medicine, and they are already used clinically for the treatment of various diseases [16, 17]. The safety issue regarding the chromosomal stability of these cells thus becomes increasingly important for future clinical applications.

Materials and methods

Cell lines and DNA extraction

HeLa cells (human cervical cancer cell line) of three different numbers of passage times were used for this study. HeLa-A was purchased from the American Type Culture Collection (ATCC, Manassas, VA), and DNA was directly extracted without cultivation. The number of passage times of HeLa-A was approximately 100 according to an attached product information sheet from ATCC. HeLa-B and HeLa-C were obtained from the Japanese Collection of Research Bioresources (JCRB, Osaka, Japan), and the number of their passage times was 122 for HeLa-B and 150 for HeLa-C.

Three different types of Caco-2 cells (human colon cancer cell line) were also used for this study. Briefly, Caco-2 was purchased from ATCC and designated as Caco-2-a, and its DNA was directly extracted without any cultivation because this DNA was regarded as a control. Caco-2-b was maintained by a commercial institution and analyzed after 63 passage times. Caco-2-c was maintained by the same commercial institution, cultured on microporous membranes (0.4 μm diameter), and analyzed after 58 passage times.

The ACBRI-519 cell line, which was derived from normal human intestinal epithelial cells, was used as a counterpart of Caco-2 cells in this study. ACBRI-519 cells were purchased from Cell System Corp. (Kirkland, WA).

Three MSCs were derived from individual bone marrow samples that were actually used clinically [16]. MSC-1 was derived from a 69-year-old female and analyzed at passage number 3 after primary culture using bone marrow. In a similar manner, MSC-2 was derived from a 16-year-old female and analyzed at passage number 3. MSC-3 was derived from a 34-year-old male and analyzed at passage number 4. MSC-4 was derived from the same individual as MSC-3, but analyzed at passage number 7.

Extraction of genomic DNA was carried out by using SepaGene (Sanko Junyaku, Tokyo, Japan) except MSCs, and genomic DNA of MSCs was extracted by using the Gentra Puregene Cell Kit (Qiagen, Hilden, Germany). Each procedure of DNA extraction was according to the manufacturer's respective protocols.

BAC aCGH

BAC aCGH analysis was carried out as described previously [7]. Briefly, 500 ng of genomic DNA from a given cell line as the test sample and 500 ng of gender-matched reference genomic DNA (Promega Corporation, Madison, WI) were labeled with cyanine3-dCTP (Perkin Elmer Inc., Waltham, MA) for reference DNA or cyanine5-dCTP (Perkin Elmer) for test DNA by random priming in 50-μl reaction volumes by using the Bioprime DNA Labeling System (Life Technologies Corporation, Carlsbad, CA) and Array Kit (Macrogen, Seoul, Korea, http://www.macrogen.com). After labeling, unincorporated fluorescent nucleotides were removed by using a QIAquick polymerase chain reaction (PCR) purification kit (Qiagen). Labeled test and reference DNAs were mixed and dissolved in hybridization solution (Macrogen) containing 100 μl Cot-1 DNA solution and 4 μl yeast tRNA solution (Macrogen). The array CGH was provided by Macrogen MAC Array KARYO 4000. This array slide had 4030 BAC clone DNAs in duplicate and covered the entire human genome with 1-Mbp resolution. The hybridization-to-wash procedure was carried out by using a Hybristation (Digilab Inc., Holliston, MA). Hybridization was carried out at 37°C for 48–72 h on the Hybristation with continuous agitation. The wash procedure was as follows: 50% formamide/2× standard saline citrate (SSC) at 46°C for 15 min, followed by 0.1% SDS/2× SSC at 46°C for 30 min, PN buffer (0.1 M Na_2PO_4/0.1% NonDiet P-40, Nakarai Tesque, Kyoto, Japan) at 37°C for 15 min, and 2× SSC at 37°C for 5 min. The array slides were scanned at 532 and 635 nm by using a GenePix4000A (Molecular Devices, Sunnyvale, CA) and analyzed by Mac Viewer software (Macrogen). The Mac Viewer software analyzed the results as follows: (1) averaged the fluorescence ratios of the replicates and calculated

the standard deviation (SD), (2) rejected individual spot data based on several criteria including weak fluorescent signals, (3) adjusted Cy5/Cy3 ratios such that ratios of the normal genomic regions were always equal to 0, despite variations in dye labeling efficiency, and (4) plotted data relative to the position of the clones on the human genome, according to July 2003, University of California, Santa Cruz cartography. In this study, all BAC aCGH analyses were confirmed to calibrate by the hybridization of the normal male DNA versus normal female DNA. The entire SD value of the $\log_2$ ratio calculated for chromosomes 1–22 was 0.07. Accordingly, DNA copy number abnormalities were defined as more than three times higher than the SD in order to account for experimental errors. For this research, a $\log_2$ ratio of 0.3 was employed to indicate abnormal differences, with the normalized $\log_2$ ratio of fluorescence intensity of over 0.3 being taken as gain and one of below −0.3 as loss.

Results and discussions

Evaluation of HeLa cells

To evaluate the chromosomal stability and instability of HeLa cells, we analyzed three different HeLa cells by BAC aCGH, as shown in Fig. 1. In the case of HeLa-A, DNA was directly extracted from ATCC HeLa cells without cultivation. HeLa-B and HeLa-C were cultured for different periods of time prior to DNA extraction (HeLa-B for 122 passages and HeLa-C for 150 passages). Novel DNA copy number loss occurred at chromosomes 3 and 13 in HeLa-C [Fig. 1a, b(i), (iii), respectively]. Moreover, at 9p13.1–p24.3, on the short arm of chromosome 9, CGH profiles showed a tendency of the DNA copy number to decrease with increased passage time [Fig. 1a, b(ii)]. Similar results were obtained for the entire regions of chromosome 1 [Fig. 1a(*)]. In contrast, the CGH profiles showed a tendency for the DNA copy number for the entire regions of both chromosomes 21 and 22 to increase with increased passage time [Fig. 1a(*)]. Additionally, Table 1 summarizes the average of $\log_2$ ratios for the above-mentioned regions obtained from BAC aCGH analysis. These results indicate that chromosomal instability including DNA copy number alterations was generated by long-term culture of HeLa cells. HeLa-C, in comparison to HeLa-A, would be distinguished as a variant of HeLa cells or might be a different cell. To summarize our analysis using BAC aCGH, continuous cultivation of HeLa cells caused a significant change at the chromosomal level. Until now, chromosomal changes in cultured cells have been recognized only empirically. If a chromosomal change occurs, it will result in a significant change at the expression level. For scientific research using cultured cells, such a change is extremely critical. Based on our present findings, we stress the importance of validation of experimental cultured cells even at the chromosomal level.

Evaluation of Caco-2 cells

This colon cancer cell line is well known to be a heterogeneous cell line and to differentiate spontaneously into small intestinal epithelial cells after its cultures have reached confluence [18–20]. Such differentiated Caco-2 cells can be cultured as monolayers on permeable filters and correlate well with the absorption system of normal intestinal cells. Therefore, Caco-2 cells are used industrially as a simulation model of intestinal drug absorption in drug discovery [15]. As described above, HeLa cells displayed chromosomal instabilities including DNA copy number alterations in a passage time-dependent manner. To evaluate the chromosomal stability including DNA copy number aberrations of Caco-2 cells, we analyzed Caco-2 cells under several different conditions by using BAC aCGH. The CGH profile for Caco-2-a, which was used as the control, is shown in Fig. 2. These cells showed no significant difference in comparison to Caco-2 cells purchased from the European Collection of Cell Cultures (ECACC, Wiltshire, UK) or from DS Pharma Biomedical Co., Ltd. (Osaka, Japan; data not shown). Caco-2-b cells, which were analyzed at passage number 63, and Caco-2-c cells, which had been cultured on the microporous membranes, showed no remarkable differences in CGH profile in comparison to Caco-2-a. Other culture conditions, such as fewer passage times than the 63 passages for Caco-2-b and use of larger diameter membrane than that used for Caco-2-c, gave similar CGH profiles (data not shown). These results indicate that the Caco-2 cell line, in comparison to the HeLa cell, is a chromosomally stable cell line, even though it was established from a cancer cell. Therefore, the Caco-2 cell line would be considered a suitable cell line for use in a validation system of intestinal drug absorption, as verified from the aspect of chromosomal stability assessed by BAC aCGH.

The ACBRI-519 cell line, which was established from normal human intestinal epithelial cells, was regarded as an alternative of the Caco-2 cell line. CGH profiles showed no significant differences between ACBRI-519 and Caco-2 cells, as also shown in Fig. 2. According to the result of BAC aCGH, ACBRI-519 and Caco-2 cells would be regarded as the same cell line. Indeed, Yamamoto et al. [21] reported that the IL-8 response to oxidative stress was almost the same between Caco-2 cells and ACBRI-519 cells. Thus, BAC aCGH can be used to recognize and to distinguish cell lines.

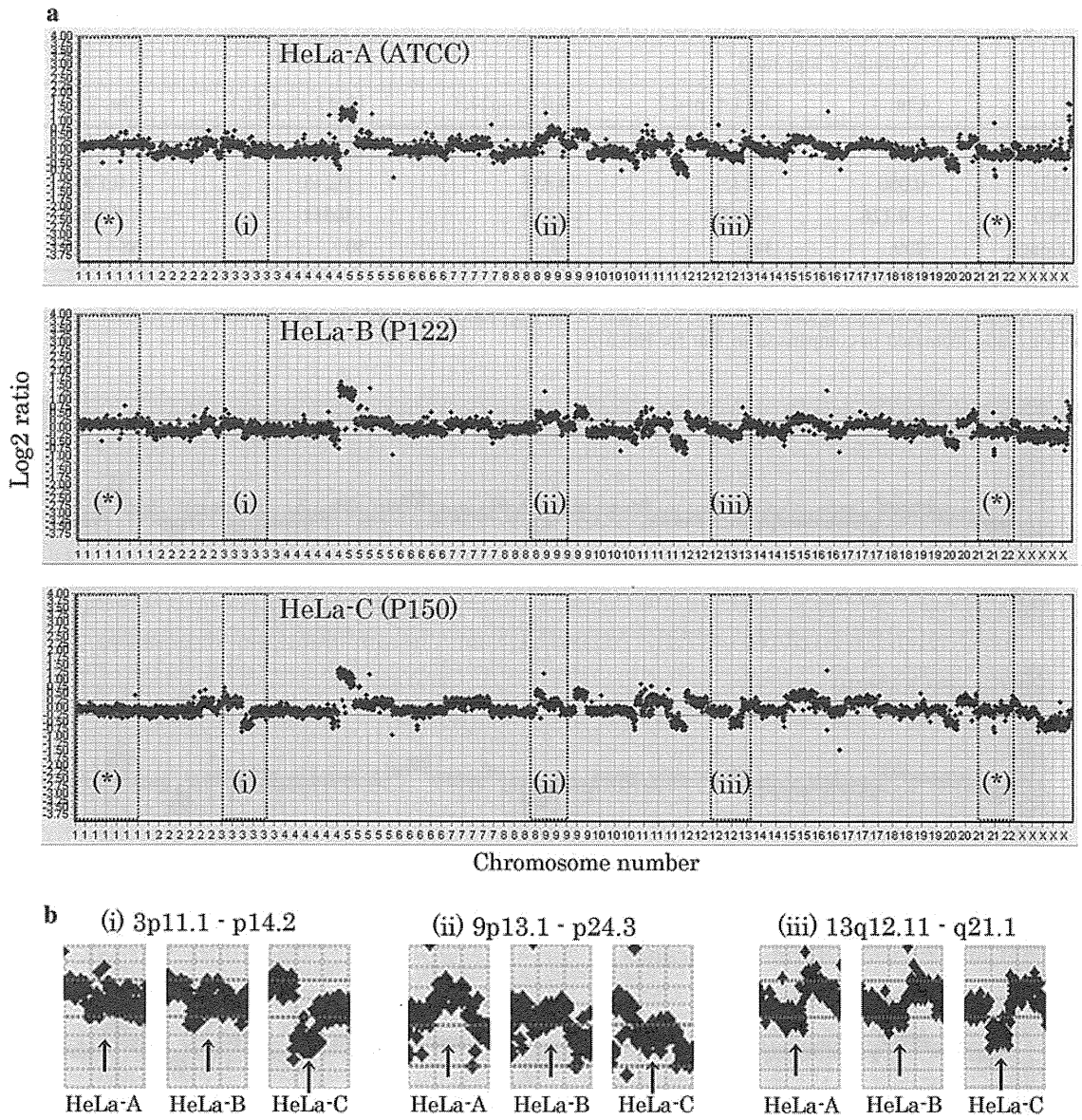

Fig. 1 BAC aCGH profiles of three HeLa cells. **a** *Upper panel* BAC aCGH profile of HeLa-A (ATCC), *middle panel* HeLa-B (JCRB, after 122 passages), *lower panel* HeLa-C (JCRB, after 150 passages). (*i*)–(*iii*) Correspond to **b**(*i*) to (*iii*), respectively. An *asterisk* indicates a tendency for DNA copy number alterations. The *ordinate* indicates the $\log_2$ ratio of Cy5/Cy3 and abscissa, the chromosome number (also applies to Figs. 1b, 2, 3). **b** Three remarkable regions of DNA copy number aberrations. *Arrows* point to regions of remarkable DNA copy number loss

Evaluation of MSCs

MSCs have been widely used clinically in the field of regenerative medicines; for instance, they are used for the treatment of osteoarthritis, bone tumor, acute myocardial infarction, and graft-versus-host disease [16, 17, 22, 23]. Because the tumorigenesis of MSCs is still a controversial issue, the safety evaluation of MSCs is very important [9–11]. BAC aCGH is a powerful method for detecting DNA copy number aberrations, which are strongly associated with tumorigenesis. In this study, we analyzed MSCs that already had been used clinically without tumor formation for osteoarthritis patients [16]. As shown in Fig. 3, the CGH profiles of MSC-1, MSC-2, and MSC-3 followed the baseline linearly; the SD values for these CGH profiles were 0.028 ± 0.060 for MSC-1, 0.043 ± 0.072 for MSC-2, and 0.029 ± 0.063 for MSC-3. In the case of MSC-4, which was passaged three more times than MSC-3, it also followed the baseline linearly (SD value was 0.018 ± 0.073). These results indicate that these MSCs did not have any chromosomal instability including DNA copy number aberrations. Therefore, BAC aCGH was able to confirm the

Table 1 Average of $\log_2$ ratios for the regions showing DNA copy number alterations in three types of HeLa cells

Region	Average of $\log_2$ ratio					
	Chr. 1	3p11.1–p14.2	9p13.1–p24.3	13q12.11–q21.1	Chr. 21	Chr. 22
HeLa-A (ATCC)	0.120	−0.114	0.581	−0.248	−0.180	−0.145
HeLa-B (P122)	0.080	−0.154	**0.337**	−0.245	−0.170	−0.105
HeLa-C (P150)	**−0.126**	**−0.635**	**0.126**	**−0.511**	*−0.146*	*−0.029*
Number of clones	299	34	63	50	68	100

Chr. indicates whole region of the chromosome; P122 and P150, analysis after 122 and 150 passages, respectively; number of clones, the number of BAC clones in the corresponding region; bold type, the value of the $\log_2$ ratio decreased in comparison to that for HeLa-A; italic type, the value of the $\log_2$ ratio increased in comparison to that for HeLa-A

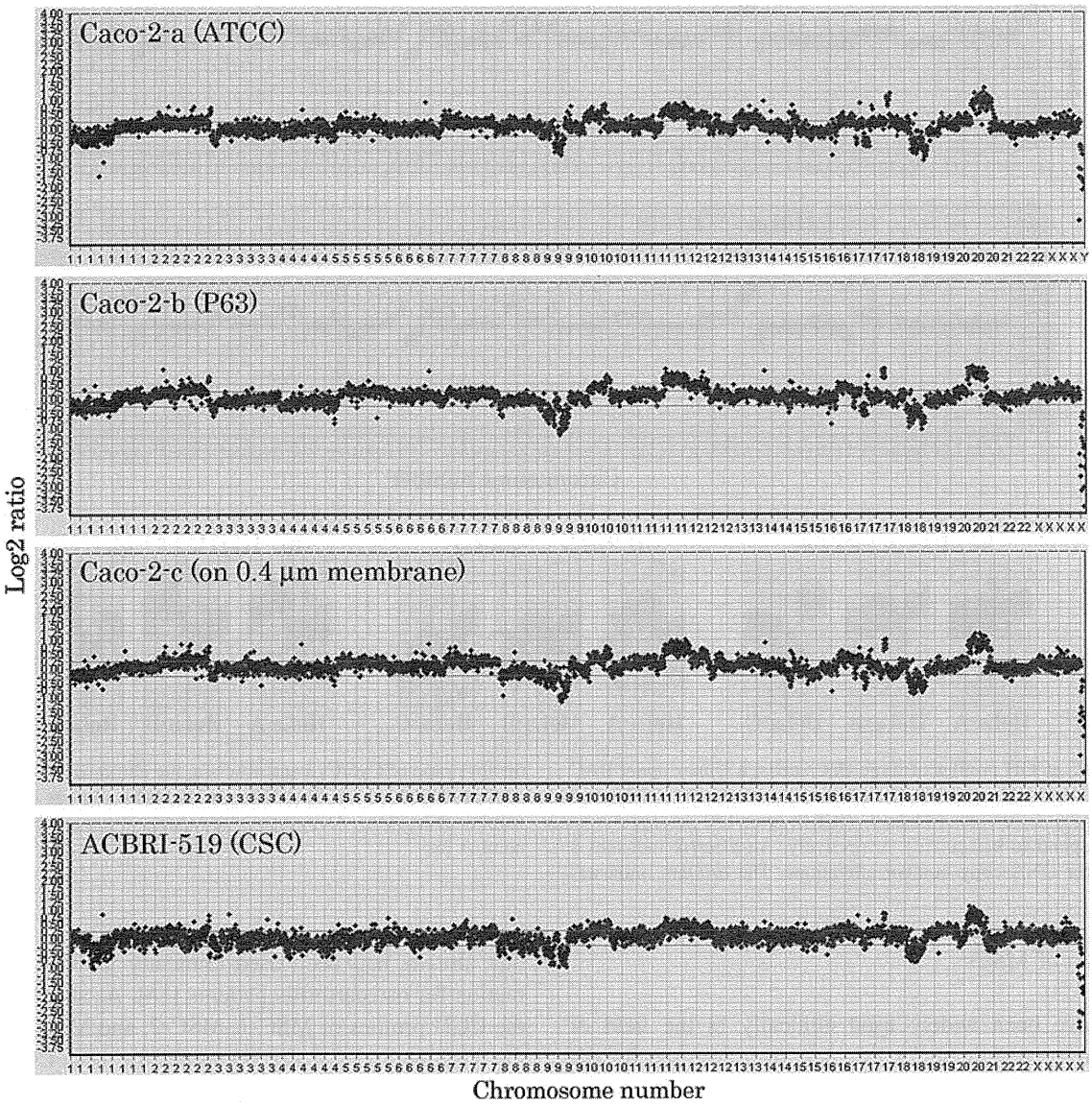

Fig. 2 BAC aCGH profiles of 3 Caco-2 cells and ACBRI-519 cells. Sequentially from the upper panel are the BAC aCGH profile of Caco-2-a (ATCC), -b (after 63 passages), -c (cultured on 0.4-μm diameter microporous membrane), and ACBRI-519 (Cell System Corp.)

safety of these MSCs at the genome level, especially DNA copy number change, which correlates well with tumorigenesis. In Fig. 3, several BAC clones that were outside the normal range (considered as normal from −0.3 to 0.3, see "Materials and methods") were possible copy number variants (CNV). These clones were confirmed as CNV loci

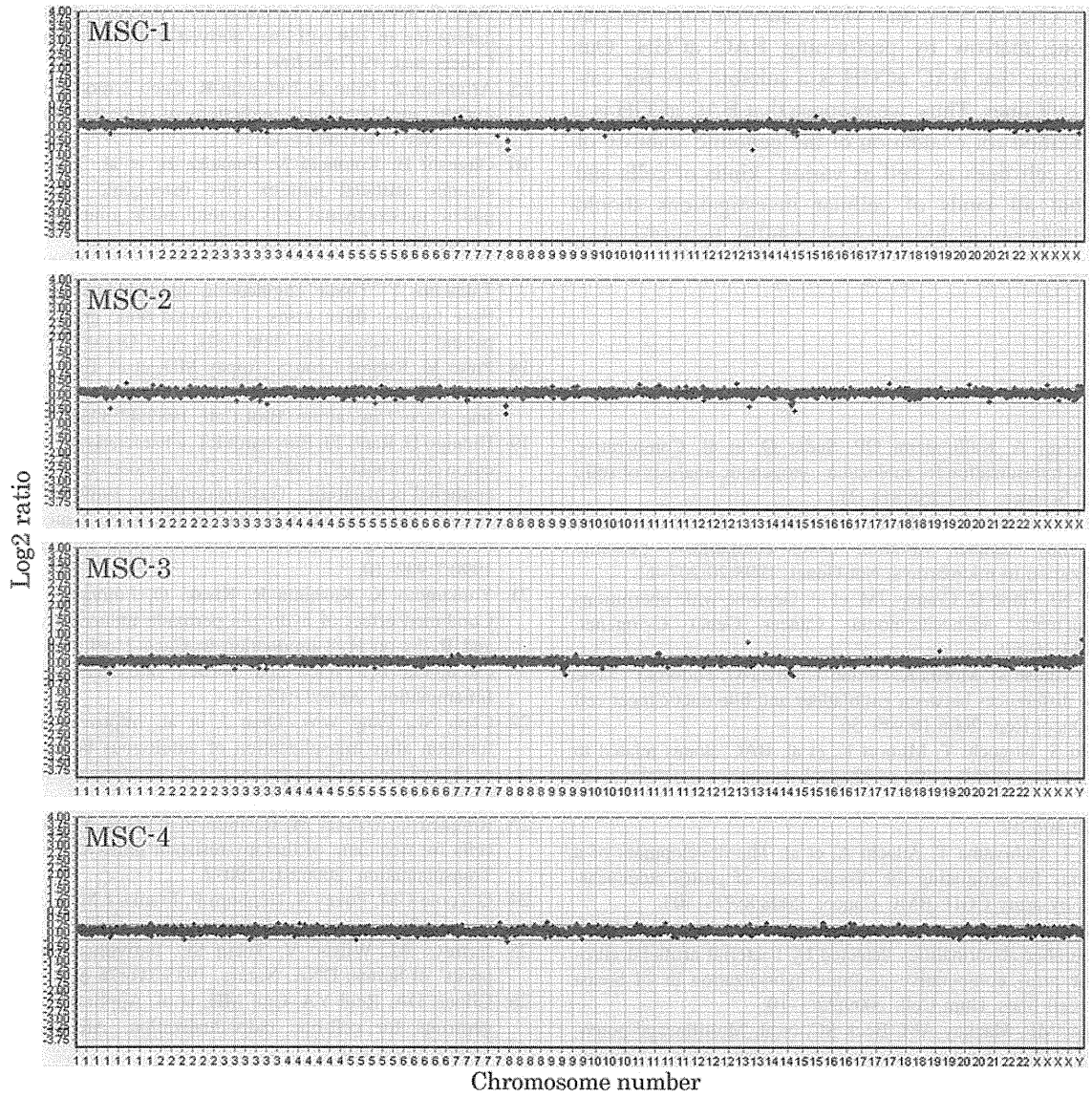

Fig. 3 BAC aCGH profiles of four clinically used MSCs. Sequentially from the upper panel the BAC aCGH profiles are shown of MSC-1 (69-year-old female after three passages), -2 (16-year-old female after 3 passages), -3 (34-year-old male after 4 passages), and -4 (derived from the same individual as MSC-3, after 7 passages)

or in their proximity (data not shown), according to the Database of Genomic Variants website of the University of Toronto (http://projects.tcag.ca/variation/).

Although established cell lines are now an essential tool in biological and clinical studies, no one has seriously questioned the reliability of such cell lines until now. Actually, most investigators have noted morphological and/or biological alterations of cell lines during long-term culture. For coping with such alterations, these cell lines have been discarded and renewed from frozen stocks after a certain number of passages. However, the substantial alterations caused by long-term culture have not been seriously considered. Validation to detect cross contamination of cell lines has been made by using various methods, such as HLA typing, DNA polymorphism, DNA fingerprinting, karyotyping, STR profiling, and SNPs [24–29]. In particular, STR profiling, which was developed for forensic sciences [30], was proposed as an international reference standard for human cell lines [28]. These methods can only detect at limited partial regions of the human genome. However, tumorigenesis is known to correlate with various chromosomal instabilities including DNA copy number changes throughout the entire human genome. Therefore, to avoid overlooking the possibility of tumorigenesis, it is necessary to validate cells by using BAC aCGH, as it can analyze all regions in the entire human genome. In this study, we investigated chromosomal stability and instability of established cell lines,

HeLa cell, Caco-2 cells, and MSCs derived from normal human bone marrow by performing BAC aCGH. Our results indicate that BAC aCGH is a suitable tool for validation of cell lines. Thus, we propose that BAC aCGH is a superior method for evaluation of the genomic stability of established cell lines as well as various kinds of cells and suggest that all kinds of cellular investigations should include validation of chromosomal stability by performing BAC aCGH.

References

1. Kallioniemi A, Kallioniemi OP, Sudar D, et al. Comparative genomic hybridization for molecular cytogenetic analysis of solid tumors. Science. 1992;258:818–21.
2. Pinkel D, Segraves R, Sudar D, et al. High resolution analysis of DNA copy number variation using comparative genomic hybridization to microarrays. Nat Genet. 1998;20:207–11.
3. Nowak NJ, Gaile D, Conroy JM, et al. Genome-wide aberrations in pancreatic adenocarcinoma. Cancer Genet Cytogenet. 2005;161:36–50.
4. Saito S, Ghosh M, Morita K, Hirano T, Miwa M, Todoroki T. The genetic differences between gallbladder and bile duct cancer cell lines. Oncol Rep. 2006;16:949–56.
5. Hirasaki S, Noguchi T, Mimori K, et al. BAC clones related to prognosis in patients with esophageal squamous carcinoma: an array comparative genomic hybridization study. Oncologist. 2007;12:406–17.
6. Furuya T, Uchiyama T, Adachi A, et al. The development of a mini-array for estimating the disease state of gastric adenocarcinoma by array CGH. BMC Cancer. 2008;8:393–403.
7. Saito S, Morita K, Hirano T. High frequency of common DNA copy number abnormalities detected by bacterial artificial chromosome array comparative genomic hybridization in 24 breast cancer cell lines. Hum Cell. 2009;22:1–10.
8. Pittenger MF, Mackay AM, Beck SC, et al. Multilineage potential of adult human mesenchymal stem cells. Science. 1999;284:143–7.
9. Alison MR, Islam S. Attributes of adult stem cells. J Pathol. 2009;217:144–60.
10. Bernardo ME, Zaffaroni N, Novara F, et al. Human bone marrow derived mesenchymal stem cells do not undergo transformation after long-term in vitro culture and do not exhibit telomere maintenance mechanisms. Cancer Res. 2007;67:9142–9.
11. Rubio D, Garcia-Castro J, Martin MC, et al. Spontaneous human adult stem cell transformation. Cancer Res. 2005;65:3035–9.
12. Gey GO, Coffman WD, Kubicek MT. Tissue culture studies of the proliferative capacity of cervical carcinoma and normal epithelium. Cancer Res. 1952;12:264–5.
13. Masters JR. HeLa cells 50 years on: the good, the bad and the ugly. Nat Rev Cancer. 2002;2:315–8.
14. Fogh J, Wright WC, Loveless JD. Absence of HeLa cell contamination in 169 cell lines derived from human tumors. J Natl Cancer Inst. 1977;58:209–14.
15. Artursson P, Palm K, Luthman K. Caco-2 monolayers in experimental and theoretical predictions of drug transport. Adv Drug Deliv Rev. 2001;46:27–43.
16. Ohgushi H, Kotobuki N, Funaoka H, et al. Tissue engineered ceramic artificial joint-ex vivo osteogenic differentiation of patient mesenchymal cells on total ankle joints for treatment of osteoarthritis. Biomaterials. 2005;26:4654–61.
17. Morishita T, Honoki K, Ohgushi H, Kotobuki N, Matsushima A, Takakura Y. Tissue engineering approach to the treatment of bone tumors: three cases of cultured bone grafts derived from patient's mesenchymal stem cells. Artif Organs. 2006;30:115–8.
18. Pinto M, Robine-Leon S, Appay MD, et al. Enterocyte-like differentiation and polarization of the human colon carcinoma cell line. Caco-2 in culture. Biol Cell. 1983;47:323–30.
19. Hidalgo IJ, Raub TJ, Borchardt RT. Characterization of the human colon carcinoma cell line (Caco-2) as a model system for intestinal epithelial permeability. Gastroenterology. 1989;96:736–49.
20. Hilgers AR, Conradi RA, Burton PS. Caco-2 monolayers as a model for drug transport across the intestinal mucosa. Pharm Res. 1990;7:902–10.
21. Yamamoto K, Kushima R, Kisaki O, Fujiyama Y, Okabe H. Combined effect of hydrogen peroxide induced oxidative stress and IL-1α on IL-8 production in Caco-2 cells (a human colon carcinoma cell line) and normal intestinal epithelial cells. Inflammation. 2003;27:123–8.
22. Chen SL, Fang WW, Qian J, et al. Improvement of cardiac function after transplantation of autologous bone marrow mesenchymal stem cells in patients with acute myocardial infarction. Chin Med J. 2004;117:1443–8.
23. Ringdén O, Uzunel M, Rasmusson I, et al. Mesenchymal stem cells for treatment of therapy-resistant graft-versus-host disease. Transplantation. 2006;81:1390–7.
24. O'Toole CM, Povey S, Hepburn P, Frankc LM. Identity of some human bladder cancer cell lines. Nature. 1983;301:429–30.
25. Jeffreys AJ, Wilson V, Thein SL. Individual-specific 'fingerprints' of human DNA. Nature. 1985;316:76–9.
26. Gilbert DA, Reid YA, Gail MH, et al. Application of DNA fingerprints for cell-line individualization. Am J Hum Genet. 1990;47:499–514.
27. MacLeod RA, Dirks WG, Matsuo Y, Kaufmann M, Milch H, Drexler HG. Widespread intraspecies cross-contamination of human tumor cell lines arising at source. Int J Cancer. 1999;83:555–63.
28. Masters JR, Thomson JA, Daly-Burns B, et al. Short tandem repeat profiling provides an international reference standard for human cell lines. Proc Natl Acad Sci USA. 2001;98:8012–7.
29. Demichelis F, Greulich H, Macoska JA, et al. SNP panel identification assay (SPIA): a genetic-based assay for the identification of cell lines. Nucleic Acids Res. 2008;37:2446–56.
30. Oldroyd NJ, Urquhart AJ, Kimpton CP, et al. A highly discriminating octoplex short tandem repeat polymerase chain reaction system suitable for human individual identification. Electrophoresis. 1995;16:334–7.

BASIC SCIENCE

Nanomedicine: Nanotechnology, Biology, and Medicine
7 (2011) 914–924

ELSEVIER

Research Article

nanomedicine
Nanotechnology, Biology, and Medicine

nanomedjournal.com

In vivo study of dendronlike nanoparticles for stem cells "*tune-up*": from nano to tissues

Joaquim M. Oliveira, PhD[a,b,c], Rui A. Sousa, PhD[a,b], Patricia B. Malafaya, PhD[a,b], Simone S. Silva, PhD[a,b], Noriko Kotobuki, PhD[c], Motohiro Hirose, PhD[c], Hajime Ohgushi, MD, PhD[c], João F. Mano, PhD[a,b], Rui L. Reis, PhD[a,b,*]

[a]*Biomaterials, Biodegradables and Biomimetics Research Group, Department of Polymer Engineering, University of Minho, Headquarters of the European Institute of Excellence on Tissue Engineering and Regenerative Medicine, Guimarães, Portugal*

[b]*Institute for Biotechnology and Bioengineering, PT Government Associated Laboratory, Braga, Portugal*

[c]*Research Institute for Cell Engineering (RICE), National Institute of Advanced Industrial Science and Technology (AIST), Amagasaki, Japan*

Received 3 September 2010; accepted 5 March 2011

Abstract

The control of stem cell differentiation to obtain osteoblasts in vivo is still regarded as a challenge in stem-cell-based and bone-tissue engineering strategies. Biodegradable dexamethasone-loaded dendron-like nanoparticles (NPs) of carboxymethylchitosan/poly(amidoamine) dendrimer have been proposed as intracellular drug-delivery systems of bioactive molecules. In this study, combination of nanotechnology, stem-cell engineering and tissue engineering is proposed in pre-programming the fate of rat bone marrow stromal cells (RBMSCs) towards osteoblasts cells and development of new bone tissue, in vivo. This work demonstrated that the developed NPs were able to be taken up by RBMSCs, and exhibited a noncytotoxic behavior in vitro. The performance of the developed dendronlike NP system for the intracellular delivery of dexamethasone was investigated by seeding the engineered RBMSCs onto starch-polycaprolactone scaffolds ex vivo, and implanting subcutaneously in the back of Fischer 344/N rats (Syngeneic), in the absence of the typical osteogenic supplements. Favorable results were observed in vivo, thus suggesting that stem cell "tune-up" strategy can open up a new regenerative strategy for bone-tissue engineering.

From the Clinical Editor: In this study, a combination of nanotechnology, stem-cell engineering and tissue engineering is proposed in pre-programming the fate of rat bone marrow stromal cells (RBMSCs) towards osteoblasts cells and development of new bone tissue in vivo.

Key words: Bone; Cytotoxicity; Internalization; In vivo; Nanoparticles; Stem cells

Advanced regenerative therapies comprise the fields of stem-cell engineering, tissue engineering and gene therapy. Cell engineering and tissue engineering have benefited from the development of novel strategies[1-3] that can stimulate and control cells' functions in vitro and in vivo. This issue is still regarded as a very appealing challenge[4-6] because there is the need to target-deliver biological agents, including differentiation factors or genetic material towards modulating from inside stem cells' behavior. We find it interesting that You et al[7] reported that surface nanotopography of polyurethane polymer functionalized with acrylate groups can enhance osteogenic differentiation synergistically with biochemical induction substance in vitro. Nevertheless, nanocarrier systems have generated a significant amount of interest in ex vivo cell maintenance and co-culturing,[8,9] and for tuning the cellular fate in vivo mainly due to their internalization ability and drug-loading capacity and to favorably modulate the solubility and pharmacokinetics of drugs.[10,11] Likewise, much attention has been given[12,13] to understanding the fundamental problem of the entry and retention mechanisms of nanoparticles (NPs) on mammalian cells as the nanodevices may be incorporated into membrane-

The authors would like to thank the financial support from Portuguese Foundation for Science and Technology (FCT, project SmartCarbo, ref. PTDC/QUI/68804/2006), through POCTI and FEDER programs. The funding provided by Canon Foundation in Europe is gratefully acknowledged. This work was also carried out under the scope of the European NoE EXPERTISSUES (NMP3-CT-2004-500283) and HIPPOCRATES (NMP3-CT-2003-505758) projects.

*Corresponding author: 3B's Research Group – Biomaterials, Biodegradables and Biomimetics, Department of Polymer Engineering, University of Minho, Headquarters of the European Institute of Excellence on Tissue Engineering and Regenerative Medicine, Taipas 4806-909, Guimarães, Portugal.

E-mail address: rgreis@dep.uminho.pt (R.L. Reis).

1549-9634/$ – see front matter © 2011 Elsevier Inc. All rights reserved.
doi:10.1016/j.nano.2011.03.002

Please cite this article as: J.M., Oliveira, et al, In vivo study of dendronlike nanoparticles for stem cells "*tune-up*": from nano to tissues. *Nanomedicine: NBM* 2011;7:914-924, doi:10.1016/j.nano.2011.03.002

bounded endosomes and fail to access the cytosolic cell targets. In this regard dendrimers have attracted growing interest as nanocarriers due to their ability to cross cell membranes.[14] Despite the interesting architecture and multivalency, it has been found[15] that high generation amine-terminated dendrimers are often cytotoxic. Many researchers have proposed the designing of dendrimers for biological and medical applications.[16,17] Dendrimer-based NPs may be biocompatible, possess high loading capacity and allow the bulk incorporation of bioactive molecules of higher molecular weights and of different chemistry while maintaining internalization and transfection efficiencies in comparison with conventional dendrimers. Still, these have not been successfully developed. We focused our attention on this fundamental problem and propose a novel surface-engineering strategy by using carboxymethylchitosan (CMCht), a natural amphoteric polyelectrolyte derived from chitosan, grafted to a low generation poly(amidoamine) dendrimer (PAMAM) backbone, with the aim of obtaining copolymers of new architectures and physicochemical properties,[18] the so-called CMCht/PAMAM dendrimer NPs. This class of nanobiomaterials has been projected to act intracellularly towards tuning in vivo the stem cells' fate. However, this remains 'proof-of-concept' with a previous report[18] showing that the surface engineering of PAMAM dendrimer NPs with the biodegradable CMCht possibly to manipulate the chemical composition and improve biocompatibility, thus avoiding the cytotoxic effects of high-generation dendrimers. Moreover, upon loading of dexamethasone (Dex), the dendrimer nanocarriers promoted the osteogenic differentiation of rat bone marrow stromal cells (RBMSCs) in vitro.[18,19] The delivery of Dex by means of using the NPs possibly a intracellular and regimented supply to stem cells within the required range of concentrations, which can be advantageous for proper osteogenic differentiation.

Here, we report on the effect of Dex-loading on the architecture, zeta potential and internalization ability of the developed NPs by RBMSCs. Transmission electron microscope (TEM), dynamic light scattering (DLS) and fluorescence techniques were carried out. To further investigate their osteogenic potential, in vitro and in vivo studies were performed combining cell and tissue engineering principles, i.e., using natural nano- and micro-polymeric systems. In vitro mineralization was evaluated by measuring the levels of calcein uptake. For the in vivo studies, Dex-loaded CMCht/PAMAM dendrimer NPs were exposed from culture media to RBMSCs during the expansion period and seeded onto the surface of starch-polycaprolactone (SPCL) scaffolds, followed by subcutaneous implantation in the back of Fischer 344 (F344/N) rats for 4 weeks. Bone formation was evaluated by microcomputed tomography (micro-CT) and morphometric analyses and histological studies (Haematoxylin & Eosin staining). Biochemical analyses denoting osteogenesis such as ALP activity, osteocalcin content and calcium assay were also carried out.

Methods

Synthesis and characterization of the NPs

Synthesis of CMCht/PAMAM dendrimer NPs was performed in a stepwise manner as described elsewhere.[18] CMCht with a degree of deacetilation of 80% and degree of substitution of 47% was linked to poly(amidoamine) dendrimers with an ethylenediamine core. First, the amine-terminated poly(amidoamine) dendrimers (PAMAM-AT) was obtained from commercial Starburst carboxylic-terminated poly(amidoamine) dendrimer (PAMAM-CT, G1.5) (Aldrich, St. Louis, Missouri), as follows: (1) an appropriate volume of PAMAM-CT was dissolved in ultrapure water to give a final concentration of 10 $mg.ml^{-1}$, and the pH of the solution adjusted to 6.5 with dilute hydrochloride acid (HCl) (Riedel de-Haen, Seelze, Germany), (2) 1-ethyl-3(3-dimethylaminopropyl) carbodiimide hydrochloride, EDC (Fluka, Buchs, Switzerland) was added to the PAMAM-CT solution at a molar ratio sufficient to modify the carboxylate residue of the dendrimers under agitation, (3) ethylenediamine (EDA) (Sigma, Steinheim, Germany) was added to the solution at a molar ratio equal to that of EDC, and (4) PAMAM-AT was produced by removing excess of EDC by dialysis using a dialysis tubing benzoylated (Sigma, Steinheim, Germany). Then, a PAMAM-ester terminated dendrimer was obtained from PAMAM-AT compound by adding an appropriate volume of PAMAM-AT (~ 8.4 mmol) and 1.14 ml of methyl methacrylate (~12.6 mmol) (Fluka) in methanol (Sigma) under agitation. The PAMAM-ester terminated compound was obtained by precipitation after 24 hours of reaction at 40°C. At last, CMCht/PAMAM dendrimer was obtained by removing the acetal to PAMAM-ester terminated compound[20] and by adding the CMCht at a ratio of 1:2 (w:w). The final solution was diluted by adding 30 ml of methanol and kept under agitation for 1 hour. After that time period, Dex-loaded CMCht/PAMAM dendrimer NPs were obtained via a precipitation route by mixing the CMCht/PAMAM dendrimer NPs with Dex at a final concentration of 5×10^{-5} M under agitation. NPs were obtained after precipitation by adding an appropriate volume of a saturated sodium carbonate, Na_2CO_3 (Aldrich) solution and cold acetone (Pronalab, Lisbon, Portugal). The precipitate was collected by filtration and dispersed in ultrapure water. The solution was dialyzed against deionized water for several days by means of using a dialysis tubing benzoylated (Sigma, St. Louis, Missouri). The NP powders were obtained after freezing the solution at −80°C and freeze-drying (Telstar-Cryodos -80, Terrassa, Spain) up to 4 days to completely remove the solvent. Fluorescent probe NPs were also synthesized using fluorescein isothiocyanate (FITC).[18] The incorporation of Dex into the CMCht/PAMAM dendrimer NPs was investigated by ^1H NMR spectroscopy. CMCht/PAMAM dendrimer NPs and Dex-loaded CMCht/PAMAM dendrimer NPs were dissolved in deuterated water, D_2O (Aldrich). The NMR spectra were obtained with a Mercury - 400BB operating at a frequency of 399.9 MHz at 50°C. The one-dimensional ^1H NMR spectra were acquired using a 45° pulse, a spectral width of 6.3 kHz and an acquisition time of 2.001 seconds. The changes on the morphology of the CMCht/PAMAM dendrimer NPs after incorporation of Dex was investigated under TEM (Philips CM-12, FEI Company, Eindhoven, The Netherlands) equipped with a MEGA VIEW-II DOCU camera and Image Software Analyzer SIS NT DOCU, as previously described elsewhere.[18] In addition, zeta potential and particle-size distribution of the NPs loaded and nonloaded with Dex were investigated at physiological and lysosomal typical

pH's using a particle-size analyzer (Zetasizer Nano ZS, Malvern Instruments, Worcestershire, United Kingdom). For this study, particle-size analyses were also performed by DLS in an aqueous solution with low concentration of NPs and using disposable sizing cuvettes. Electrophoretic determinations of zeta potential were investigated in citrate buffer (pH 3) and phosphate buffered saline (PBS) of pH 7.4 solutions, using the universal 'dip' cell. Zeta potential was also investigated in water. For further details see Supplementary Information.

SPCL scaffolds

A blend of starch and poly-ε-caprolactone from Novamont (Novara, Italy) 30/70 (w/w) was used to produce fibers of SPCL by melt spinning using a modular co-rotating twin screw extruder. SPCL scaffolds with 5 mm diameter and 4 mm height were obtained by fiber bonding as reported elsewhere.[19,21] Before in vitro and in vivo studies, the CMCht/PAMAM dendrimer NPs, the Dex-loaded CMCht/PAMAM dendrimer NPs and SPCL scaffolds were sterilized in an ethylene-oxide gas atmosphere.

Cells isolation and luminescent cell viability assay (ATP quantification)

For the in vitro cell culturing studies, RBMSCs were isolated from femora of 7-week-old male Fischer 344/N rats (SLC Inc., Hammamatsu, Japan), and expanded in T75 cm^2 culture flasks in the presence of Eagle's minimum essential medium (MEM) (Nacalai Tesque, Kyoto, Japan) supplemented with 15% fetal bovine serum (FBS), (JRH Biosciences, Tokyo, Japan) and 1% antibiotic/antimycotic (A/B) (Nacalai Tesque) solution, the so-called MEM complete medium. First, the animals were sacrificed following the protocol approved by Ethics Committee at the Tissue Engineering Research Center, Amagasaki, Japan. The femora were collected, the marrow flushed out and marrow cells from each shaft were transferred into a T75 cm^2 culture flask (BD Biosciences Discovery Labware, Bedford, Massachusetts) and expanded under standard culturing conditions. The culture medium was changed within a 3-day period to remove nonadherent cells, followed by changing the culture medium every 2 or 3 days until reaching about 80% confluence. RBMSCs were trypsinized with 1 ml of 0.05% tripsin-0.53 mM EDTA (Invitrogen, Carlsbad, California) solution, and incubated for 3 minutes at 37°C. Complete MEM culture medium was added and RBMSCs (passage 1, P1) were centrifuged at 900 rpm for 5 minutes. Then, supernatant was aspirated and cells resuspended with 10 ml of complete culture medium. Cell counting was performed using an automated counter (Cell Counter Sysmex F-520, Kobe, Japan). Viability of RBMSCs was analyzed with a NucleoCounter (Chemometec, Allerød, Denmark), prior seeding.

To investigate possible cytotoxicity of the NPs, a cell-viability assay was carried out. RBMSCs were seeded (subcultured) to each well of a 96-well tissue culture polystyrene (TCPS) plate at a cell density of 5×10^3 cells.ml^{-1}. Serial dilutions (1, 0.1, 0.01 mg.ml^{-1}) of CMCht/PAMAM dendrimer NPs and Dex-loaded CMCht/PAMAM dendrimer NPs were prepared using the MEM complete culture medium, and RBMSCs cultured with the respective media for 24 and 72 hours. A latex rubber extract was used as the positive control for cellular death. After each time point, the ATP content was measured by means of performing a CellTiter-Glo luminescent cell-viability assay (Promega Corp., Madison, Wisconsin). Luminescence was measured in a microplate reader (Wallac ARVOsx 1420, Perkin-Elmer Life and Analytical Sciences, Shelton, Connecticut). All experiments were carried out in triplicate using 4 replicates per experimental condition (n=12).

In vitro cellular uptake ability of the dendronlike NPs

RBMSCs were isolated and expanded as aforementioned. Then, cells were subcultured in a 6-well (1×10^5 cells.$well^{-1}$) and TCPS coverslips in 24-well TCPS plates (2×10^4 cells.$well^{-1}$) for analysis under FACS and fluorescence microscopy, respectively. For fluorescence microscopy, RBMSCs were cultured in a MEM complete culture medium supplemented with the FITC-labelled Dex-loaded CMCht/PAMAM dendrimer NPs and MEM complete culture medium with the FITC-labelled CMCht/PAMAM dendrimer NPs at a final concentration of 0.1 mg.ml^{-1}, for the period of 12 hours for 14 days. For FACS analysis, RBMSCs were cultured in the presence of FITC-labelled Dex-loaded CMCht/PAMAM dendrimer NPs and FITC-labelled CMCht/PAMAM dendrimer NPs at a final concentration of 0.01 mg.ml^{-1}. All experiments were carried out in triplicate. After each time period, the RBMSCs were fixed with 4% formalin (Nacalai Tesque) and incubated with Texas Red-X phalloidin (Molecular Probes, Invitrogen) and Hoechst 33258 (Invitrogen) for staining the actin filaments of cytoskeleton and nuclei of cells, respectively. We followed the protocols provided by the supplier, with few modifications. The specimens were observed under a fluorescence microscope (Olympus IX70, Olympus Co. Ltd., Tokyo, Japan).

Before FACS analysis each well of the 6-well plate was washed with PBS and cells released from substratum as described above. After centrifugation at 900 rpm for 5 minutes, RBMSCs were resuspended in 0.5 ml of complete culture medium and passed through cell strainers.[22] Propidium iodide (Nacalai Tesque) was added to each sample to determine the number of live cells. Then, RBMSCs were loaded in a FACSCalibur flow cytometer (BD Biosciences Immunocytometry Systems, San Jose, California) and analyzed with a minimum of 10,000 events counting. All experiments were carried out in triplicate and following the protocol described elsewhere.[18]

In vitro assessment of osteogenesis and viability assay

RBMSCs (P1) were cultured in a TCPS 24-well plate at a cell density of 2×10^4 cells.$well^{-1}$ for 24 hours. After that time, the culture medium was replaced by the different culture medium, and RBMSCs cultured for up to 14 days. The effect of the concentration of Dex-loaded CMCht/PAMAM dendrimer NPs on the RBMSCs osteogenic differentiation was investigated as previously reported elsewhere, using positive and negative controls for osteogensesis.[18] The degree of mineralization was qualitatively and quantitatively investigated as described by Uchimura et al.[23] The method consists of the culturing of the RBMSCs in the presence of 1 μg.ml^{-1} of calcein (Dojindo Laboratories, Kumamoto, Japan), which is incorporated in the mineralized ECM and allows us to investigate the calcium deposition, after 1, 7 and 14 days. The fluorescence of calcein

incorporated into the mineralized matrices was both visualized and quantified in a image analyzer equipment (Typhoon 8600 Variable Mode Imager, Amersham Biosciences, Piscataway, New Jersey) using a 526 nm short pass filter. Afterward, the fluorescence of the incorporated calcein was also observed under a fluorescence microscope (Olympus IX70, Olympus Co., Ltd.). All experiments were carried out 3 times using a minimum of 4 replicates per experimental condition (n=12).

In vivo study

RBMSCs were expanded in different culture media namely, MEM, MEM supplemented with Dex and MEM supplemented with the Dex-loaded CMCht/PAMAM dendrimer NPs. RBMSCs at different cell number (1×10^6 and 2×10^5) were seeded onto the surface of the SPCL scaffolds, cultured overnight in MEM complete medium for cell adhesion, and then constructs were implanted subcutaneously. Seven-week-old male F344/N rats (Syngeneic), same as donor substrain and age, were anesthetized by intraperitoneal injection of pentobarbital (Nembutal, Dainippon Pharmaceutical Co. Ltd., Osaka, Japan) at a final concentration of 3.5 mg per 100 g of body weight. In each rat, 3 or 4 skin incisions (each 1 cm length) on the dorsal midline below the ear were made. Each RBMSCs-SPCL constructs was implanted subcutaneously (1.5 to 2 cm away from the midline at both right and left sides) into the respective pocket and skin sutured. As a negative control, we used SPCL implants without RBMSCs. All animals received their usual dietary regimen and no prophylactic medication was administered post surgery. After 4 weeks' implantation, the animals were sacrificed with an overdose of anesthetic and the implants were retrieved. All experiments were carried out 3 times using a minimum of 3 implants per condition.

Micro-CT and morphometric analysis

New bone formation in the explants was evaluated using a high-resolution micro-CT Skyscan 1072 scanner (Skyscan, Kontich, Belgium) with a resolution of pixel size of 6.59 μm and integration time of 1.7 ms. The x-ray source was set at 40 keV and 250 μA. Approximately 400 projections were acquired over a rotation range of 180° with a rotation step of 0.45°. Data sets were reconstructed using standardized cone-beam reconstruction software (NRecon v1.4.3, SkyScan). The output format for each sample was 500 serial 1024 × 1024 bitmap images. A representative data set of 250 slices was segmented into binary images with a dynamic threshold of 220-255 (grey values) to assess de novo bone formation. The same representative volume of interest (VOI) was analysed for all the samples. These data sets were used for morphometric analysis (CT Analyser, v1.5.1.5, SkyScan) and to build the 3D models (ANT 3D creator, v2.4, SkyScan). The morphometric analysis included scaffold characterization such as porosity and interconnectivity, histograms and new bone formation quantification. The distribution of this new bone formation in the scaffolds was assessed by 3D virtual models that were created, visualized and registered using both image-processing softwares (CT Analyser and ANT 3D Creator). After μ-CT analysis the explants were prepared as described in the Supplementary Information following a standard protocol[24] for further histological observation.

Histological analysis

After micro-CT analysis, the explants were decalcified with K-CX solution (Falma Co., Tokyo, Japan) for histological analysis. First, the explants were dehydrated in an ascending series grade ethanol/water solution (from 90–100%) for 19 hours followed by washing 3 times with xylene. Then, explants were immersed in paraffin at 62°C and allowed to solidify at -5 °C. Slides were prepared by cutting the explants into sections 5 μm thick using a microtome and mounted in a microslide glass (Matsunami Glass Ind. Ltd., Osaka, Japan). Paraffin was melt by placing the slides in the oven at 71°C for 20 minutes and allowed to let cool down at room temperature (18–21°C). The remnant paraffin was then subsequently removed from slides by immersion in hexane for 5 minutes (S.T. Chemical Co. Ltd., Tokyo, Japan), and in a ethylene/propylene mixture (Clear Plus, Falma Co., Tokyo, Japan) for 3 minutes. Then, slides were immersed 3 times in 100% ethanol for 2 minutes each time of immersion. For the Haematoxylin & Eosin (H&E) staining, slides were sequentially transferred to a 90% ethanol and then to a 70% and washed with tap water. It followed the staining steps and mounted for observation as described elsewhere.[10] All experiments were carried out in triplicate using 3 replicates per experimental condition (n=9).

Analyses of biochemical parameters

ALP activity and osteocalcin content were measured to evaluate osteoblast differentiation in vivo. Before the assay the explants were washed with Ca and Mg-free PBS solution. Then, explants were processed as previously reported.[19,24] Standards were prepared with p-nytrophenol, pNP. Triplicates were made for each sample and standard and experiments repeated 3 times (n=9). Absorbance was read at 405 nm (Wallac ARVOsx 1420, Perkin-Elmer Life and Analytical Sciences), and sample concentrations were read from the standard graph. Enzyme activity was expressed either as nmol of pNP released/explant/30 minutes. The remnant of each sample used for the ALP assay of the explants was treated with a 20% formic acid solution and stored at 4°C for 2–3 days. Afterward samples were centrifuged at 15,000 rpm and the supernatant was passed through a Sephadex G-25 column (GE Healthcare, Uppsala, Sweden). The samples were subsequently concentrated for performing the enzyme-linked immunosorbent assay (ELISA). A rat osteocalcin EIA kit (N° BT-460, Biomedical Technologies Inc., Stoughton, Massachusetts) was used following the instructions provided by the supplier. Data were read off from the standard curve obtained with human osteocalcin and expressed as ng of deposited osteocalcin per explant. As an index of mineral bone formation, deposited calcium in the explants was quantified as described by Kim et al[25] with minor modifications. Statistical analysis was carried out as described in the Supplementary Information.

For calcium determination, explants were rinsed with Ca and Mg-free PBS solution and 0.2 ml of 1N HCl solution per explant was added. The tissues were chopped before being placed on an orbital shaker to extract calcium for 12 hours. Then, mixtures

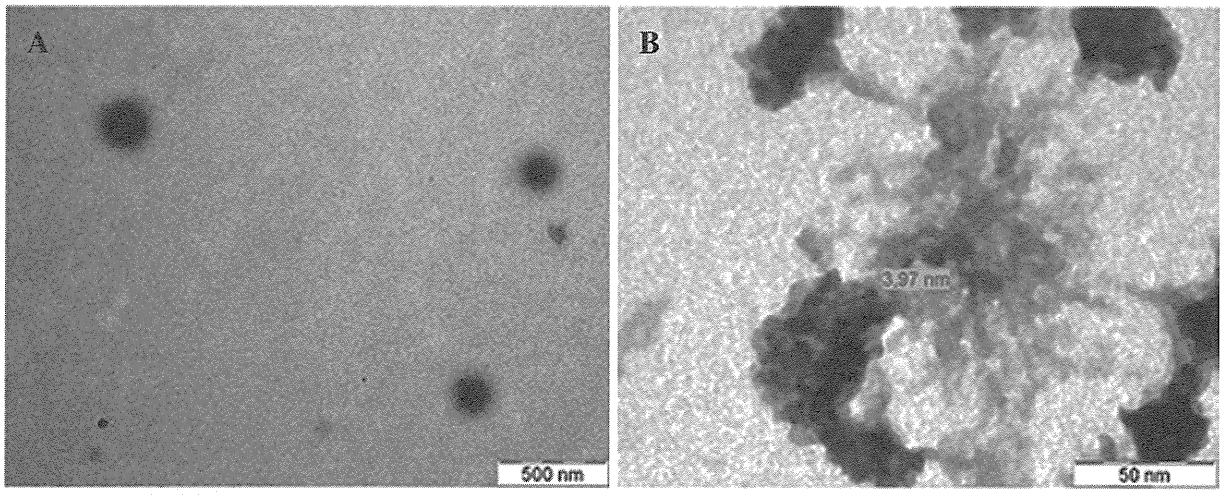

Figure 1. Characterization of the nanoparticles. Representative TEM images of the CMCht/PAMAM dendrimer NPs **(A)**, and Dex-loaded CMCht/PAMAM dendrimer NPs **(B)**.

were centrifuged at 15,000 rpm for 10 minutes and supernatants were assayed (o-cresolphthalein complexation color development method) using a commercial calcium assay kit (Calcium C-test, Wako Pure Chemical Industries, Osaka, Japan). Calcium content was determined by measuring the absorbance at 570 nm. All experiments were carried out in triplicate using 3 replicates per experimental condition (n=9).

Statistical analysis

Statistical differences were analysed using the GraphPad Prism software (GraphPad Software Inc., La Jolla, California). One-way analysis of variance (Tukey's multiple comparison test) was performed and statistical significance was defined as $P < 0.05$ for a 95% confidence interval (P value: *** < 0.001; ** < 0.01; * < 0.05).

Results

In the present work, ^{1}H NMR analysis was carried to investigate the loading of Dex into the Dex-loaded CMCht/PAMAM dendrimer NPs (Figure S1). The spectrum shows the typical signals from CMCht, PAMAM dendrimers and Dex. It is possible to observe small singlets at 1.14, 1.28 ppm and 1.86 ppm from CH_3 and CH_2 groups, and a doublet at 7.55 ppm and 7.96 ppm, which are attributed to the chemical shifts of the protons attached to C1 atoms and to aromatic ring (∗) of Dex, respectively. By its turn, to evaluate the morphology of the NPs upon loading with Dex, TEM analysis was performed (Figure 1). From images we can observe that the loading of Dex can affect the morphology of the NPs. In fact the formation of dendronlike NPs instead of the typical nanosphere-like morphology is revealed. Zeta potential and particle size of the CMCht/PAMAM dendrimer NPs and Dex-loaded CMCht/PAMAM dendrimer NPs were also measured by DLS (Table S1). Results showed that the hydrodynamic diameter of the CMCht/PAMAM dendrimer NPs in PBS (pH 7.4), increased upon Dex loading, and the value of the NPs' zeta potential changed from −32.8 to −27.3 mV (experiments carried out in water).

In vitro cell culture studies were performed to investigate possible cytotoxicity and uptake of NPs by RBMSCs. Fluorescence microscopy images of RBMSCs cultured in the presence of FITC-labeled and Dex-loaded CMCht/PAMAM dendrimer NPs revealed that the NPs are taken up by RBMSCs, after 12 hours (Figure 2). The cell-viability assay of RBMSCs cultured in the presence of different culture medium revealed that NPs are noncytotoxic over RBMSCs at concentrations bellow 1 $mg.ml^{-1}$ (Figure S2). FACS analysis was also performed after culturing the RBMSCs in the presence of the FITC-labelled NPs for up to 14 days (Figure S3 and Table S2). FACS analysis revealed increasing levels of fluorescence associated with cells after incubation of RBMSCs with CMCht/PAMAM dendrimer NPs. The fraction of live cells cultured in the presence of FITC-labeled Dex-loaded CMCht/PAMAM dendrimer NPs do not significantly differ from that of controls. This is a good indication that NPs do not elicit any cytotoxic effect over RBMSCs. The osteogenic ability of Dex-loaded CMCht/PAMAM dendrimer NPs was investigated by qualitatively and quantitatively determining the levels of calcein uptake (Figure 3 and Figure S4). Results demonstrated that mineralization can only occur in cultures in which RBMSCs were supplemented with Dex-loaded CMCht/PAMAM dendrimer NPs in comparison with to positive control (osteogenic medium). Moreover, it can be seen that NP concentration significantly affects mineralization, i.e., superior mineralization occurs when using 0.01 $mg.ml^{-1}$ Dex-loaded CMCht/PAMAM dendrimer NPs in comparison with that for 1 $mg.ml^{-1}$ Dex-loaded CMCht/PAMAM dendrimer NPs. The osteogenic studies are supported by phase contrast and respective fluorescence microscopy images of RBMSCs after culturing in different culture medium and in the presence of calcein for 14 days (Figure S5). In the Figures 5S, *C-E*, it can be observed the typical mineral nodule formation in RBMSCs cultures that were exposed to Dex, both from culture media or from the Dex-loaded CMCht/PAMAM dendrimer NPs.